Spring 2018

SYNTHESIS AND EVALUATION OF ACETYLCHOLINE MOLECULARLY IMPRINTED POLYMERS

Nathaniel Donald Thiemann
Trinity College, Hartford Connecticut, nathaniel.thiemann@trincoll.edu

TRINITY COLLEGE

SYNTHESIS AND EVALUATION OF ACETYLCHOLINE MOLECULARLY IMPRINTED POLYMERS

BY

Nathaniel Thiemann

A THESIS SUBMITTED TO

THE FACULTY OF THE NEUROSCIENCE PROGRAM

IN CANDIDACY FOR THE MASTER'S OF ARTS DEGREE IN NEUROSCIENCE

NEUROSCIENCE PROGRAM

HARTFORD, CONNECTICUT

May 10, 2018

SYNTHESIS AND EVALUATION OF ACETYLCHOLINE MOLECULARLY IMPRINTED POLYMERS

BY

Nathaniel Thiemann

Master's Thesis Committee

Approved:

_____

Timothy Curran, Thesis Advisor

_____

William Church, Thesis Committee

_____

Charles Swart, Thesis Committee

_____

Sarah Raskin, Director, Neuroscience Program

Date: _____

Abstract

Polymers imprinted with acetylcholine during synthesis were prepared in order to evaluate their potential for implementation as a novel recognition element in acetylcholine biosensors. Biosensors, such as the glucose monitor, are used to rapidly detect and quantify a target analyte. Acetylcholine biosensors have already been produced using enzymatic recognition elements, but they are currently expensive and plagued by short viability. Molecularly imprinted polymers are not only cheap and durable, but have also been successfully used as a recognition element in biosensors for other analytes. Therefore, computational tools were used to rationally design acetylcholine molecularly imprinted polymers. Three chemicals, itaconic acid, acrylamide, and methacrylamide were identified during this process, because they had an unusually energetically favorable tendency to form a complex with acetylcholine *in silico*. These three chemicals were used to attempt polymer synthesis in 7mL glass vials, but successful formation was only observed with acrylamide and methacrylamide polymers. A new batch of the two types of polymers was then synthesized and subjected to a binding capacity assay. All polymers were loaded with an 80mM acetylcholine solution, washed three times with deionized water, then washed three times with a designated elution solution. Each sample collected from the polymers during the assay was analyzed via flow injection analysis mass spectrometry. Imprinted polymers generally retained a higher percentage of the acetylcholine they were loaded with than the non-imprinted control polymers. Furthermore, non-imprinted polymers generally had very little acetylcholine left to release after being washed with deionized water, while imprinted polymers still had acetylcholine bound after being washed with deionized water. These results indicated a strong possibility that there was a successful imprinting effect for acetylcholine in the imprinted polymers. A methanol/acetic acid mixture also proved to be the most efficient method

for removing acetylcholine from polymers amongst the four elution solutions that were tested. The experimental protocol needs further refinement procedurally and analytically to reliably quantify the acetylcholine in unknown samples from the binding assay. If enough progress is made though, then it could be possible to use the polymers to measure acetylcholine in a solution. This would open up the possibility for acetylcholine molecularly imprinted polymers to be used as an alternative recognition element in acetylcholine biosensors, which have applications in medicine, research, and agriculture.

Significance Statement

Other peer reviewed works have given precedent to the logic that chemicals that form low stabilization energy complexes with a template *in silico* are ideal candidates for synthesizing a polymer that is molecularly imprinted for the template *in vitro*. The current work sought to test this precedent through the rational design, and then synthesis, of polymers that were molecularly imprinted for acetylcholine. Two of the three chemicals highlighted by the rational design process were successfully used to synthesize polymers. Furthermore, the polymers imprinted for acetylcholine showed a markedly higher percent of acetylcholine retention compared to polymers not imprinted for acetylcholine in a binding capacity assay. Although the quantitative method used in the current work needs further refinement to accurately quantify unknown amounts of acetylcholine, the results qualitatively indicate the efficacy of the rational design process used. The successful behavior of the acetylcholine imprinted polymers indicated the high efficacy of the rational approach taken to designing them. This fact is very important, since only free and publicly available software was used during the process. Most importantly, it seems possible that the produced acetylcholine molecularly imprinted polymers have the potential to be adapted for the rapid detection and quantitation of acetylcholine in aqueous solutions. Such quantitative

capabilities would augment the ability to study acetylcholine related questions in fields such as agriculture, ecology, and medicine.

Introduction

Part 1 – Biosensors

Biosensors are used to rapidly detect and quantify a target analyte, they typically consist of a biological component or biomimetic approach (Wilson, 2005; Hajek, 2001; Lin Ding, 2008; Nakamura, 2003; Su, 2011). The two main components of every biosensor are the recognition element and the transduction element, which are in physical contact. The recognition element is responsible for detecting the presence of the target analyte in the sample. Recognition elements can be biological such as an antigen, protein, or cell; or non-biological such as a chelator, quantum dot (Igor, 2003), or nanomaterial (Nicholls, 2011). The transduction element, which is in physical contact with the recognition element, translates the detection of the target analyte into a quantity by means of a specifically designed scheme. These schemes are all designed to measure a signal like voltage, frequency, or impedance and translate any changes in that signal into a change in concentration of the analyte. The components in a biosensor can be biological or synthetic materials designed to have bio-mimetic properties.

The blood glucose monitor, first invented in 1956 by Clark, is the most commonly known biosensor (Clark, 1962). The contemporary blood glucose monitor incorporates the enzyme, glucose oxidase, as its recognition element. The protein is immobilized on an amperometric transduction element, which set up to measure the change in voltage as a function of enzyme mediated glucose oxidation. The biosensor quantifies the amount of glucose in the sample as a function of that change in voltage. There are now many biosensors that utilize the same paired enzyme recognition and amperometric transduction scheme. In fact, such biosensors have

already been made for dopamine (DA), serotonin (5-HT), and other chemicals that are easily oxidized.

Biosensors that have a capability to detect and quantify ACh in a sample have been engineered as well. These biosensors primarily use the coupled pair of enzymes, acetylcholinesterase (AChE) and choline oxidase (ChOx), as a recognition element in conjunction with an amperometric transduction element (Khan, 2013). Two enzymes are needed for the recognition element, because the chemical structure of ACh is highly resistant to oxidation. AChE is used to first hydrolyze ACh into acetic acid and choline. The resultant choline is then oxidized by ChOx, and the resulting change in extracellular voltage is recorded by a nearby electrode. A function can then be made that translates the change in oxidation to change in extracellular voltage, which corresponds to the amount of choline, and subsequently ACh, is in a sample, Due to ACh in a sample being quantified as a function of choline oxidation, these ACh biosensors are really another method of indirectly measuring ACh. Nonetheless, current ACh biosensors feature limits of detection (LoD) capable of detecting physiological relevant levels of ACh in a sample (Khan, 2013). Furthermore, ACh biosensors can be used in a more robust variety of experiments than alternatives such as LC-MS/MS analysis alone.

Despite the increased viability for measuring ACh in different settings afforded by ACh biosensors, they are far from perfect First of all, there is an inherent problem with relying on electrochemical sensing techniques, such as measuring oxidation, to quantify a target analyte *in vivo*. Such techniques are subject to unwanted noise generated by oxidation of other electroactive chemicals besides the target analyte, like the ubiquitous ascorbic acid (Guan, 2012). Biosensors in general also still struggle with electrode fouling, poor spatial and temporal resolution, and poor sampling frequency (Khan, 2013). ACh biosensors suffer from their own unique problem as

well, due to how difficult it is to directly measure ACh with electrochemical detection or UV-VIS spectrophotometry. In typical ACh biosensors the oxidation of choline by ChOx is dependent upon the prior hydrolysis of ACh by AChE. The need for two enzymatic reaction to occur in order to generate a signal that can be recorded, thus negatively impacting temporal resolution of ACh biosensors. Since two different kinds of proteins need to be immobilized on ACh biosensors, the number of recognition sites for ACh are also halved compared to biosensors that can be made with one enzyme or other type of uniform recognition element. Less recognition sites per area, reduces the sampling frequency per area of the ACh biosensor, negatively affecting their temporal resolution. Although spatial and temporal resolution in molecularly imprinted polymers utilized in biosensors are not exactly stellar, they are at least much less expensive to prepare than immobilizing proteins. Furthermore, the immobilization of biological components in an extracellular environment negatively affects the proteins' stability, and subsequently shortens the biosensor's viability. Therefore, functional ACh MIP are a potential cheap and durable alternative recognition element compared to recognition elements utilizing immobilized AChE and ChOX.

Part 2 - Acetylcholine

ACh was discovered in 1913 by the scientist Henry Dale (Tansey, 2006). At the time, little was known about the critical roles that neurotransmitters, like ACh, play in biological systems. However, Dale's discovery was a major step in a cascade of discoveries that has culminated in our current understanding of chemical signaling in biological systems. It is now known that cholinergic signaling is involved in voluntary movement, maintaining homeostasis, memory, cognition, and other important biological functions within living organisms. ACh is

also a potential biomarker for Alzheimer's Disease (Hyo Geun, 2014), depression (Noah, 2010), and other health related disorders (Nemeroff, 2012; Yarnall, 2011; Kaltsatou, 2015; Kimura, 2015; Jarrett, 2018). Furthermore, human pollution has given rise to studies of the effects of our waste on the cholinergic signaling of multiple species such as humans (Costa, 2014), beluga whales (Ostertag, 2018), and dogs (Costa, 2014).

There are so many unknown mechanisms by which ACh elicits its effect(s) on many of the physiological systems it has been implicated in thus far. These mechanisms need to be mapped out in order for the scientific community to truly comprehend phenomena such as consciousness (Woolf, 2011), or to effectively treat neurodegenerative pathologies (Soreq, 2015). Therefore, an improved understanding of the cholinergic system would likely have wide reaching impact on fields like agriculture, medicine, and more (Suriyo, 2015; Uteshev, 2016). However, the primary problem with studying ACh currently lies in how difficult it is to detect and quantify the neurotransmitter signaling from biological systems in real time with current available techniques (Khan, 2013).

ACh is an ester of acetic acid and choline (Figure 1) that is is rapidly hydrolyzed by AChE both pre- and post-synaptically (Zackheim, 2003; Khan, 2013). Since ACh has no significant light absorbing chromophore, the concentration of ACh in an aqueous solution cannot be directly measured through ultraviolet – visible (UV-Vis) spectroscopy (Dunphy, 2003). In fact, there is currently no method available that allows for the direct detection of ACh (Nirogi, 2010). Measuring ACh indirectly used to require using an enzymatic assay to then measure the resultant metabolite with either electrochemical detection or UV-vis spectroscopy. Alternatively, one could also have used isotope labelled ACh, which could then be measured via nuclear magnetic resonance, infrared spectroscopy, or mass spectrometry (Perry, 2009).

Figure 1 - Chemical Structure of Acetylcholine

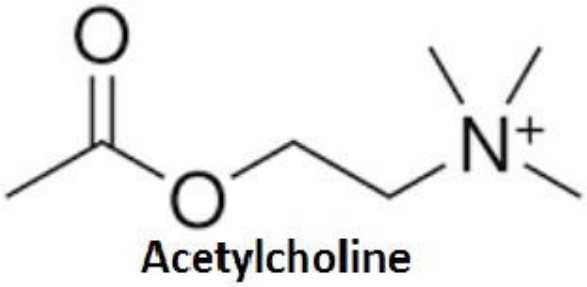

Figure 1, acetylcholine (ACh) is an ester of the two biomolecules choline and acetate. The molecule has no chromophore and is highly resistant to oxidation, making it difficult to measure through popular approaches like UV-VIS spectroscopy or electrochemical detection. Recent advancements have given rise to the quantification of ACh with LC-MS/MS analysis, and even more recently FIA-MS analysis.

These indirect techniques for quantifying ACh are very expensive in terms of the materials and labor required to use them. For instance, functional magnetic resonance imaging (fMRI) can be used to track cholinergic signaling *in vivo*, but requires access to very expensive equipment (Kimura, 2015). Furthermore, the number of tasks and environments that people want to study cholinergic signaling in far exceeds what can be studied are limited due to the physical limitations of the fMRI. For terms of price and quantitative the currently favored technique for quantifying ACh is to use liquid chromatography (LC) separation in conjunction with tandem mass spectrometry (MS/MS) detection (Dunphy, 2003). LC-MS/MS analysis allows for the highly sensitive quantification of ACh in a sample, with no need for pre-treatment of the sample. Furthermore, multiple ionization schemes can be used in the MS/MS detection, such as fast-atom bombardment, thermospray ionization, and electrospray ionization (ESI). However, out of these different ionization schemes, the ESI method is generally preferred. In ESI, a high voltage is applied to a sample in order to create an aerosol, which helps to prevent macromolecules within

the sample from fragmenting during ionization. Fragmentation generates unwanted noise in the detector, and weakens the signal of the molecule being measured, which makes experimental data harder to analyze. Although the LC-MS/MS technique is a highly sensitive for the quantification of ACh within a sample, it is largely inadequate for many of the instances in which scientists seek to study ACh *in vivo*. This is primarily because AChE hydrolyzes ACh so rapidly. Since scientists cannot instantly collect microdialysis samples typically used in LC-MS/MS studies, it is hard to be certain they are truly representative of the cholinergic signaling event that was being studied (Nirogi, 2010). These drawbacks to the LC-MS/MS technique have led to the search for a more robust technique to quantify ACh *in vivo*.

Although it is actually quantitatively worse than LC-MS/MS, flow injection analysis mass spectrometry (FIA-MS) is one currently available alternative to LC-MS/MS (Nanita, 2015). FIA-MS is a methodically simpler process than LC-MS/MS, that can be used to sample larger populations easily, but still reliably quantify a target analyte. The primary difference between the two techniques is the FIA-MS technique does not use a LC column, whereas LC-MS/MS technique does. This one change greatly decreases the separation of analytes typically seen in LC-MS/MS, which is facilitated by recent advances in sampler detection sensitivity. The increase in sensor sensitivity is what allows samples to be directly injected into the valve with no need for separation (Nanita, 2015). Although it can be used quantitatively, the FIA-MS process is not as sensitive or selective as LC-MS/MS. Therefore, for experiments where proof of concept is necessary rather than definitive quantitative results, FIA-MS is a viable alternative to LC-MS/MS.

Part 3 - Molecularly Imprinted Polymers

Alternative recognition elements should be experimented with to fully explore the possible avenues for improving ACh biosensor performance. Non-biological recognition elements can function similarly to the biological recognition elements used in ACh biosensors thus far, but are cheaper to isolate, and more resistant to non-biological environments (Hillberg, 2008). In the specific case of the ACh biosensor, replacing two proteins with one homogenous ACh recognition element could be a way to further improve spatial and temporal resolution of currently available from ACh biosensors. The increase in overall resolution would be due to a higher density of recognition sites per area available, and the ability directly measure ACh rather than a metabolite of enzymatic activity. Luckily, the growing field of nanomaterial engineering lends itself to exploring both of these options.

Nanomaterials are artificial materials that have been manipulated to have biomimetic or otherwise special phenotypic properties (Nicholls, 2011). These properties arise from a unique chemical structure or organization at the nanoscale, hence the name nanomaterials. Some specific purposes for which nanomaterials have been synthesized include: separation of molecules from various types of solutions (Ahmadi, 2011; Alexander, 2006; Khairi, 2015), drug delivery (Puoci, 2007), protein crystallization (Saridakis, 2011), scaffolding in tissue engineering (Suntornnond, 2016), imparting special phenotypic properties such as toughening (Askarinejad, 2015), signal recognition/transduction (Lattach, 2012), and antibody production (Nicholls, 2011). One recently developed nanomaterial even recreated the spatula like hairs that allow geckos to adhere to sheer vertical surfaces. This nanomaterial allowed a 70kg person to cling, like a gecko, to a sheer vertical glass wall (Hawkes, 2015). Such a biomimetic approach is not a singularity, molecularly imprinted polymers also typically take inspiration from the physical phenomenon observed in nature.

Molecularly imprinted polymers (MIPs) are a type of nanomaterial, that can feature intrinsic recognition elements to special phenotypic qualities (Algieri, 2014). MIPs made for element recognition have high specificity and affinity for their imprinted template. MIPs have been imprinted to templates ranging in size from single molecules to entire cells (Alexander, 2006) Although the materials and methodology used for their synthesis vary greatly, MIPs meant for template recognition typically feature several ingredients pre-polymerization: the template, functional monomer(s), solvent, cross-linking agent, and initiating agent. The template is the element for which the polymer is desired to have the capacity to recognize. Functional monomers are essentially the building blocks of the MIP, and form a complex with the template that will be cast into the recognition site. For this reason, functional monomers that can form reversible non-covalent interactions with the template are ideal. The porogenic solvent is a chemical that both the chosen template and functional monomer are miscible in. Cross-linking agents are used to link together the template-functional monomer complexes into a single continuous polymer upon initiation. The initiating agent triggers the polymerization process, which can be a catalyst (Hawkins, 2006), the cross-linking agent itself, UV-radiation, or temperature change (Alexander, 2006).

Some archetypal MIPs of note include: multi-layer membranes (De Luca, 2011), nanofilms (Jimenez-Solomon, 2016), sol-gels (Liu, 2016), hydrogels (Hadizadeh, 2013), and xerogels (Wach, 2013). Saridakis et al., in particular, synthesized hydrogels using the functional monomer acrylamide in water to prepare a MIP that was functional in aqueous solution (Saridakis, 2011). Many types of MIPs are unable to operate in aqueous solution, due to only being functional in organic solution. However, utilizing hydrogels allowed this group to bypass this problem and develop a highly effective technique for protein isolation. Studies like this

provided a blueprint for how to synthesize an ACh MIP that could function in water, and how to collect quality empirical data.

The types of MIPs, and the ways in which they can be synthesized, are indeed numerous. However, the diversity of syntheses that have been thought of is dwarfed by the sheer number of possible templates in comparison. Just in the last few years MIPs have been synthesized for notable templates such as: 17β-estradiol (Wei, 2007), benzylparaben (Asman, 2015), bovine serum albumin (Liu, 2016), cholate salts (Yañez, 2010), cocaine (Piletska, 2005), diazinon (Bayat, 2014), fenitrothion (Barros, 2014), homovanillic acid (Diñeiro, 2006), lactose (Hadizadeh, 2013), 3,4-methylenedioxymethamphetamine (MDMA) (Ahmadi, 2011), theophylline (Sun, 2006), tryptophan (Prasad and Rai, 2012), and urea (Chen, 2011). One extremely pertinent example of a reported MIP was made by Suedee et al. for the recognition of serotonin and dopamine. Suedee et al. synthesized an MIP with recognition sites selective for both the neurotransmitters, which showed they could be used to conduct competitive assays (Suedee, 2008). This unique example of a specialized assay for dopamine and serotonin highlighted the as of yet unexplored potential for MIPs in the field of neuroscience.

An extensive search for an ACh MIP that consisted of a non-biological recognition element with a non-amperometric transduction element yielded no positive results. However, molecular imprinting techniques had been used to immobilize AChE within an MIP for the purpose of protein isolation (Demirci, 2015). Nevertheless, there is potential for an ACh MIP to serve as a more robust recognition element in ACh biosensors, while also lending itself to alternative transduction schemes. An ACh MIP could offer one of the first true ways to directly measure ACh in a sample. Furthermore, it has been shown that MIPs are a consistently cheaper and more stable option than protein immobilization for the synthesis of a material with

recognition capabilities (Ahmadi, 2011). Finally, an ACh MIP could possibly provide much needed improvement in terms of spatial and temporal resolution by increasing recognition site homogeneity absent by necessity in contemporary ACh biosensors. Therefore, ACh biosensors with an ACh MIP for a recognition element could be more useful for *in vivo* studies, water or food quality monitoring, and environmental studies.

Despite lacking any prior mention of an ACh MIP, some lessons can be learned from previous studies on MIP synthesis. First, MIPs have been made previously for an ionic template. One of the earliest examples of an ionic template MIP was actually back in the 1970's, when MIPs were made for copper, cobalt, zinc, and cadmium ions (Nishide, 1977). This group reported that the MIP efficiency was largely dependent on the interaction between the template and functional monomers used. It has also been shown that it is best to use a crosslinking-agent to functional monomer ratio of 80%:20% for certain syntheses (Algieri, 2014). Such a ratio typically ensures adequate mechanical stability, and good recognition performance in the produced polymer. However, it is also important to consider the unique purpose (i.e. extraction, signal transduction, etc), and preferred operational environment when attempting to synthesize MIPs (Wei, 2006). Factors that can have a major impact on these functions are the very chemicals used to make MIPs. Therefore, the solvent, template, functional monomer, cross-linking agent, and initiator must all be based upon the desired function and operational environment of the final product.

For example, the ratios of all the chemicals being used must be relatively appropriate, to ensure adequate size and distribution of the imprinted recognition sites. It is also important to note that there are optimally no side reactions between the chemicals used, as that would also negatively affect the formation of the polymer (Wei, 2006). For this reason, experiments

typically only use one species of functional monomer in MIP synthesis. However, it is inevitable that many factors come into play when designing MIPs with a high selectivity for a target analyte. Therefore, it is best to treat each MIP subjectively and take the time to optimize each of these factors on a case by case basis. Until recently, the fastest method to optimize all these factors was through bulk polymerization methods, which are very expensive, labor intensive, and wasteful of valuable resources (Nicholls, 2011).

Part 4 – Rational Design of MIPs

Recent advancements in technology have provided researchers with computation tools to design MIPs have in an affordable, eco-friendly, but expedient manner (Nichols, 2009; Shoravi, 2014). These approaches allow for scientists to theoretically screen a library of chemicals for their suitability in a variety of roles. This screening saves precious resources from being wasted in bulk polymerizations. Several groups have set the precedent that a template-functional monomer complex with the lowest binding energy complex *in silico* is usually the optimal functional monomer when synthesizing MIPs *in situ* (Ahmadi, 2011; Pavel, 2006). It seems that -COOH and -CH_2OH functional groups often play a large role in the most favorable template-functional monomer complexes (Pavel, 2006). Due to their successful implementation and growing efficiency, the use of computational tools to design MIPs is growing at a fast pace.

Although computational tools have been used by pharmaceutical companies to develop new pharmacological agents for years, their adaptation to synthesis of MIPs is relatively new. Nevertheless, there is already a large assembly of peer reviewed material available where scientists have utilized computational approaches to detail the intermolecular interactions between a template and functional monomer (Barros, 2014; Diñeiro, 2006; De Luca, 2011; Nicholls, 2009). Some higher end computational chemistry software can even factor in possible

solvents and cross-linking agents when optimizing the chemicals for use in synthesis of MIPs (Ahmadi, 2011). These software help scientists predict chemical phenomena involved in MIP synthesis at a molecular level, which provides more efficient strategies for MIP design. It is important to note that there is a significant amount of trade-off between the accuracy of a computational chemistry calculation and the cost-efficiency of doing so. Or in other words, more accurate calculations are typically more expensive to run in terms of computational time (Wei, 2006).

Molecular dynamics is one computational chemistry strategy that is commonly used to compute meaningful metrics for the synthesis of MIPs (i.e. equilibrium geometry, Snyder polarity index, dielectric constants). Molecular dynamic calculations utilize Newtonian functions to compute the potential energy of a molecular system. The potential energy of the system is described by a force field, which is a stepwise integration of the Newtonian laws of motion meant to predict atomic positions at the global potential energy minimum. Molecular dynamics can also be used to determine the optimum solvent for use in polymerization of MIPs (Nicholls, 2009). Since molecular dynamics utilize Newtonian functions they can suffer from accuracy, especially in systems where the Newtonian function ends up not being linear (Crouch, 1997). Since the plot of total energy for many compounds is not linear (consider how favorability alters as you rotate substituents about a bond), this causes Newtonian functions to have limited applicability in calculating the stabilization energy of large electron systems. This barrier can often be overcome with either good logic or more computational power, but the latter option drastically reduces the benefit of increased efficiency that makes computational approaches appealing (Foster, 2009).

Molecular modeling has been very useful in computational modeling, but is lacking in terms of capability to accurately predict electronic structure of large electron systems. *Ab initio* computational methods have been developed in recent years to address this issue (Young, 2001). The term *ab initio* refers to performing a computation from the start, or in other words the Schroedinger equation. The Schroedinger equation is a differential equation that combines wave theory and particle theory, but is so complex that it cannot be truly solved for systems with more than one electron. One particularly popular derivative of *ab initio* computational approaches includes density functional theory. Density functional theory then applies the electron density of an entire system to solve a simplified version of the Schroedinger equation. Density functional theory is considered a derivative of *ab initio* calculations, because it solves an *ab initio* problem using semi-empirical parameters, rather than starting from scratch. A typical correlational function used in density function theory is the Beck 3 parameter Lee Yang Parr (B3LYP) correlation functional, which takes 3 parameters to input the semi-empirical data for the calculation of the electron density of a system. Even using semi-empirical values, approximations must be made to solve the Schroedinger equation for systems with more than one electron.

These approximations include the Born-Oppenheimer, Hartree-Fock, and linear combination of atomic orbitals. The Born-Oppenheimer approximation assumes nuclear movement is zero, thus making the repulsion from nuclei constant. The Hartree-Fock approximation assumes that each electron in a system moves independently of one another, which allows the presence that each electron feels from other electrons to be simplified into one constant field. Finally, the linear combination of atomic orbitals sets the total wave function of an atom or molecule equal to the product of one electron wave functions, or in other words the

wave function for hydrogen. With these approximations and an appropriate basis set, it is possible to perform a highly accurate approximation of the Schroedinger equation for large electron systems ranging between 50-100 atoms (Crouch, 1997). A basis set is used to determine what atomic orbitals to use in linear combination of atomic orbitals, and can greatly affect the results of a density functional theory (DFT) calculation. Typically, the smallest basis set that can be used with reliable results is the 6-31G* basis set (Crouch, 1997).

Part 5 - Synthesizing an ACh MIP recognition element

In a previous study, DFT calculations were performed to screen a library of functional monomers for their potential to form a complex with ACh in a vacuum. This library consisted of the chemicals acrylamide, acrylic acid, itaconic acid, methacrylamide, and methacrylic acid (Figure 2). The quantum calculator, General Atomic and Molecular Electronic Structure System (GAMESS), was used to calculate the equilibrium geometry of all the prepared ACh -functional monomer complexes. GAMESS is a semi-empirical program, that can be used to run *ab initio* calculations with customizable parameters. For instance, GAMESS can be used to compute transition structures, reaction coordinates, vibrational frequencies, and electrostatic potential in three dimensions. GAMESS is also parallelized for use on multiprocessor computers, and was run using server time donated by the group ChemCompute. The results from density functional theory calculations performed by GAMESS were analyzed with the visualization software MacMolPlt, and used to determine the lowest stabilization energy of the screened ACh -functional monomer complexes. MacMolPlt is designed for displaying the output of GAMESS calculations as animations, and can also be utilized to visualize electronic properties or interactions.

Figure 2 – Library of Functional Monomers Analyzed With the Quantum Calculator GAMESS

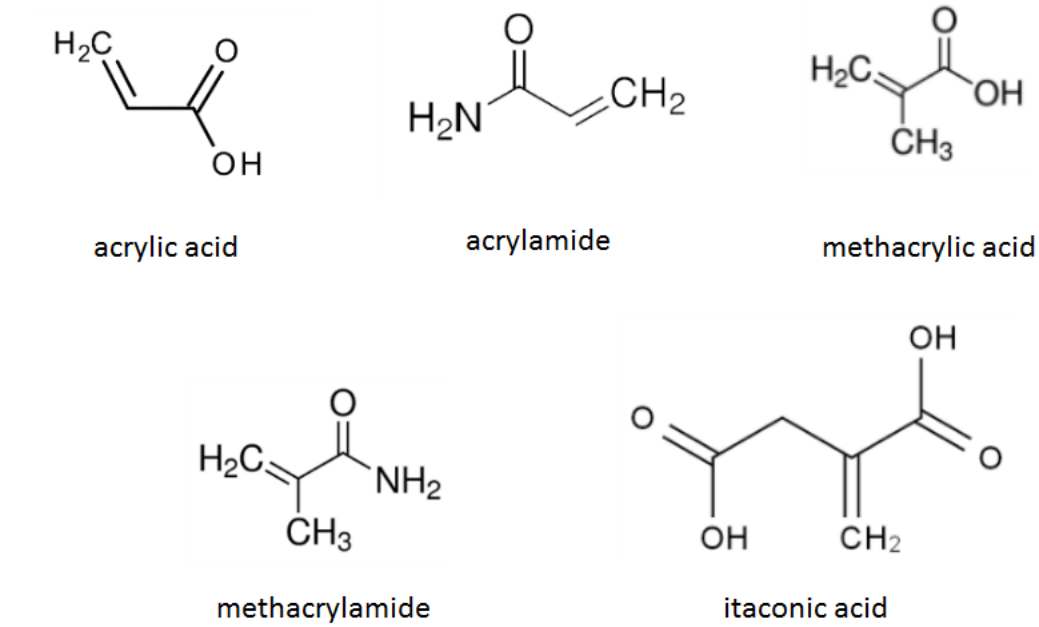

Figure 2 - The functional monomer library consisting of (from left-right, top-down) acrylic acid, acrylamide, methacrylic acid, methacrylamide and itaconic acid. These chemicals were chosen because they had been previously used in the successful synthesis of other molecularly imprinted polymers. All the monomers chosen featured a functional group that could participate in ionic and hydrogen bonding interactions. Specifically, carboxylic acids and amide functional groups were used because they are very common in amino acids. Therefore, monomers that featured these functional groups were maybe more likely to engage in biomimetic behaviors.

The results of the computational studies performed indicated the functional monomers acrylamide, methacrylamide, and itaconic acid were identified as the most likely to form an energetically favorable to complex with ACh in isolated conditions. These three chemicals were used to attempt polymer synthesis in 7mL glass vials, but successful formation was only observed with acrylamide and methacrylamide polymers. A new batch of the two types of polymers was then synthesized and subjected to a binding capacity assay. FIA-MS analysis was used to measure the amount of ACh in samples collected from different stages of a binding capacity assay (Hawkins,2006; Dunphy, 2003). These analyses were used to quantify the ACh in each sample recovered from the binding capacity assay. Standards with known concentrations were used to construct a calibration curve that could be used to somewhat reliably estimate the

concentration of ACh in each sample from the binding capacity assay. Both the percent of ACh in total and the percent of ACh per treatment were then calculated and analyzed. A fully functional ACh MIP that could be used to quantify ACh in a sample in real time. It would also lay the groundwork for future experiments to explore the potential as a recognition element in an ACh biosensor. These biosensors could be used in research, medical devices, prosthetics, or water/food quality sensors.

Materials and Methods

Experimental Design

The results of Sussman et al. were validated by doing a docking study of an AChE crystal structure that was found on Protein Data Bank (PDB, PDB code: 1EEA). Once we analyzed the results of the docking study and confirmed they were dependable, we chose functional monomers that have noted use in synthesizing MIPs. PDB, pubchem, and peer reviewed articles were used to obtain lattice constants for each functional monomer and ACh. These lattice constants were used to create input files of ACh -functional monomer complexes with appropriate parameters to create a supercell. A quantum calculator was then used to run density functional theory calculations to see which complex of functional monomers with ACh had the lowest stabilization energy. It was expected that the lowest energy complex will serve to make the best performing ACh MIPs.

Acrylamide, methacrylamide, and itaconic acid were chosen for this experiment based on their theoretical potential to participate in hydrogen bonding and ionic interactions with ACh in a vacuum (See results, Table 2). First, ACh imprinted hydrogels were synthesized using itaconic acid, acrylamide, or methacrylamide as the functional monomer. The protocol used in the

experiment was a modified version of the one proposed by Hawkin's et al. to isolate bovine hemoglobin (Hawkins, 2004). However, attempted syntheses only yielded a polymer in the acrylamide and methacrylamide samples. Afterwards, syntheses were only conducted with acrylamide or methacrylamide. Control acrylamide and methacrylamide non-imprinted polymers (NIPs) were synthesized in the same manner as experimental MIPs, but without ACh.

Multiple elution solutions were tested to identify the best way to remove ACh template molecules from experimental MIPs. Four different solutions were tested to see which maximized ACh recovery in a binding capacity assay. The ultimate goal of the binding capacity assay was to show that MIPs had a highly specific affinity for ACh compared to NIPs. The "Load" treatment of the assay was an 80mM ACh stock solution, which was added during synthesis for experimental MIPs and after synthesis for 20 minutes on a stir rack for control NIPs. All "Wash" treatments consisted solely of DIH_2O, which was applied for 20 minutes on a stir rack for all polymers. Once all samples from the binding assay were collected, the ACh in each sample was quantified using FIA-MS analysis. If there was no imprinting effect, then ACh would freely elute during the "loading" and/or "washing" stages. However, if there was an imprinting effect, then ACh would primarily elute during the "elution" stage and minimally during the other two stages (Hawkins, 2004).

Reagents

acetylcholine chloride (AChCl), glacial acetic acid (AcOH), hydrochloric acid (HCl), itaconic acid, methacrylamide, and methanol (MeOH) were purchased from Fischer Scientific (NJ, USA). Acrylamide, ammonium persulfate (APS), N,N-methylenebisacrylamide (NMBA), and N,N,N′,N′-tetramethylethylenediamine (TEMED) were purchased from Bio-Rad (CA, USA). Tris(hydroxymethyl)aminomethane (Tris) and potassium chloride (KCl) were obtained

from Fischer Chemical (NJ, USA). Sodium dodecyl sulfate was purchased from LifeTechnologies (MD, USA). Deionized water (DIH_2O) was provided by Trinity College (CT, USA).

Equipment

Micropipettes and transfer pipettes were provided by Trinity College (CT, USA). Microcentrifuge tubes (5mL), round flat-bottomed sample vials (7mL), and 2mL screw top autosampler vials were purchased from Fischer Scientific (NJ, USA). Measurements of mass were made using scales accurate to the mg in Trinity College's quantitative chemistry lab. The ACh in each assay sample was quantified by using a shimadzu LC controller with a 4000 QTrap LC-MS/MS for FIA-MS analysis in the quantitative chemistry lab at Trinity College. Vacuum purging was also performed using a motorized vacuum pump from Trinity College's quantitative chemistry lab. Server access and time were provided by professor Mark Perri of Sonoma State University.

AutoDock Analysis

The program AutoDock (http://autodock.scripps.edu/, RRID:SCR_012746) was downloaded along with an crystal structure of *Electrophorus electricus* AChE with ACh bound to it from PDB (http://www.rcsb.org/pdb/explore.do?structureId=1EEA, RRID:SCR_006555). A new file for the receptor and ligand were saved in the same directory. The protein had all the water molecules in the structure removed and hydrogens added wherever needed. A grid of the protein was made and AutoDock was run via the command prompt in order to dock ACh in all the possible sites it could bind to the protein. The results were saved in the same directory as the accompanying intermediate files. The results of the docking study were analyzed with the visualization software PyMOL (https://www.pymol.org/, RRID:SCR_000305). The site with the

most favorable binding energy was further analyzed with the program Maestro (https://www.schrodinger.com/maestro). This analysis was done so that the chemical interactions between ACh and involved amino acid residues could be determined and cleanly visualized.

GAMESS Analysis

The quantum chemistry calculator GAMESS (http://www.msg.ameslab.gov/gamess/, RRID:SCR_014896) was used in order to calculate the equilibrium geometry, or lowest stabilization energy, for each ACh -functional monomer complex. The program Avogadro (https://avogadro.cc/) was used to prepare the input files for GAMESS analysis. To prepare the input files, the structure for ACh was retrieved from the crystal structure for AChE previously used in the AutoDock analysis. The crystal structures for the functional monomers methacrylic acid, acrylic acid, methacrylamide, and acrylamide were retrieved from Pubchem (https://pubchem.ncbi.nlm.nih.gov/, RRID:SCR_004742). The crystal structure for another functional monomer, itaconic acid, was replicated from the data provided by Graham et al. in 1997.

In each GAMESS input file, a copy of the ACh crystal structure was in a complex with one to three functional monomer(s). The complex was put into a unit cell, which was organized so that the edges of the cell were always ~10Å away from the nearest Cartesian coordinate of an element within it. Before saving the parameters for the file, the complexes were relaxed via energy optimization with the MMFF94s force field (4 steps per update, steepest descent, fixed/ignored atoms were movable) for 10-15 seconds to ensure the molecules were in a somewhat favorable confirmation. Afterwards, the files were saved as GAMESS input files meant to calculate the equilibrium geometry of the complex with the following parameters: Cartesian coordinates, B3LYP correlational functional, 6-31G(d,p) basis set, in gas phase.

Density functional theory calculations for each complex were performed three times to ensure results. The energies for the template (ACh) and each functional monomer were also calculated using density functional theory. A total of three calculations was also performed for each individual molecule (i.e. ACh and each functional monomer being screened).

The GAMESS calculations were conducted using servers provided by ChemCompute (https://chemcompute.sonoma.edu/index.html), which is a website that allows students and researchers to easily run computational chemistry software for free. The input files were uploaded to the web via a user interface in the researcher mode on ChemCompute. Each job was run using 24 computer cores at a time, and went until the total energy converged to a global minimum or the allocated memory was exceeded. For files whose calculations exceeded the allocated memory, the Cartesian coordinates for the complex from the most recent iteration of the density function theory self consistent field calculation were turned into a new input file. By doing this, it was possible to append the progress of incomplete calculations together, thus allowing for some of larger complexes (i.e. the 1:3 complexes) to be completed. Once completed, the calculations were retrieved from ChemCompute, and analyzed using the program MacMolPlt (https://brettbode.github.io/wxmacmolplt/). MacMolPlt was used to visualize the chemical formations and interactions of the lowest stabilization energy for each complex. The energy for each trial was recorded with Microsoft excel, which was also used to do statistical analysis of the density functional theory results.

Equation 1 - Calculation of Complex Stabilization Energy Using Calculated Total Complex and Molecular Energies

$$\Delta E = E_{(template\ -\ monomer)} - \{E_{(template)} + \sum E_{(monomer)}\}$$

Equation 2 – Conversion of Stabilization Energy from Atomic Units to Kilojoules per Mole

$$(\Delta E * 1\ a.u). * \{(627.51\ kcal/mol) / (1\ a.u)\} * \{(4.184\ kJ/mol) / (1\ kcal/mol)\} = (\Delta E * 2625.50\ kJ/mol)$$

Solution Preparation

A stock solution of AChCl (100mM) was prepared in DIH_2O, then diluted as needed into 10mM, 1mM, 100µM, 10µM, 1µM and 100nM standard solutions via series dilution. Stock solutions of stock 80 mM AChCl solution (ACh loading solution), 10%SDS:10%AcOH (w/v, SDS/AcOH), 9:1 MeOH:AcOH (v/v, MeOH:AcOH), KCl (0.1M), 50mM Tris-HCl (pH 8.9, Tris-HCl), 5% TEMED (v/v), 10% APS (w/v), and 20%MeOH(v/v) were prepared with DIH_2O water except for the MeOH:AcOH solution.

Acetylcholine Molecularly Imprinted Polymer Synthesis

Polymers were synthesized in 7mL flat bottomed glass vial with 4mL DIH_2O, 48mg AChCl, 24mg NMBA, and 216mg of functional monomer. The functional monomer was either acrylamide, methacrylamide, or itaconic acid. Once prepared, the solution was ultrasonicated for 1min then vacuum purged for 5min to remove oxygen, which could otherwise interfere with matrix formation (Khimji, 2013). Afterwards, 40µLof TEMED and APS stock solutions were added to the solution. The polymers were then sealed with a snap cap, and allowed to polymerize for 12 hours at 23°C.

Binding Capacity Assay

Four groups of twelve polymers were synthesized. Each group consisted of four different kinds of polymer, which were acrylamide MIPs, methacrylamide MIPs, acrylamide NIPs, and methacrylamide NIPs. There were three of each of polymer in every group. Group A was treated with the SDS/AcOH stock solution during elution treatments, while groups B, C, & D were

treated with MeOH:AcoH, KCl, & Tris-HCl stock solutions, respectively. There were two inconsistencies in how polymers were treated. First, MIPs were loaded with ACh stock solution during synthesis, but NIPs were loaded with ACh stock solution after synthesis then allowed to equilibriate for 20 minutes on a stir rack. Second, NIPs from groups A and B were loaded with 3 mL volumes, but otherwise all post synthesis treatments were 2mL volumes. MIPs needed to be synthesized with ACh to potentially be imprinted, and they needed to be loaded with the same solution as NIPs. Therefore, MIPs were loaded with 48mg of ACh at synthesis. However, NIPs besides those mentioned in the second inconsistency were loaded with 24mg of ACh. After the NIPs were allowed to equilibriate with the ACh loading solution for 20 minutes, all MIPs and NIPs were washed with 2mL DIH_2O for another 20 minutes. The DIH_2O wash was repeated twice in the same manner, then polymers were treated in the same fashion with their respective elution solution three times as well. All treatments were collected after application and saved in appropriately labeled microcentrifuge tubes for FIA-MS analysis.

FIA-MS Analysis

FIA-MS analysis was used to analyze binding capacity assay samples as well as ACh standards. The LC-MS/MS was run on LCMS-No Oven profile, with no column, and a probe height of 5mm. All injections were made in volumes of 20µL, 0.1 ml/min, and maintained at a 23°C temperature. The mass spectrometer (MS) was operated with 20%MeOH mobile phase, in Q1 MS scan type for an extracted ion peak at 146.2 m/z, for a duration of 2min, and using ESI. ESI was performed at a voltage of 4.5 kV, with no external heat source active. The area under the signal generated at 146.2m/z was integrated from 0.2min to 1.2min for all assay samples and ACh standards. The log of the average area of each ACh standard was then plotted against the log of the respective standard's [ACh] in order to perform a linear regression analysis of the

relationship. The resulting trendline was a calibration curve that was used to roughly estimate the concentration of unknown assay samples based on their integrated area at peak 146.2m/z. The amount of ACh each polymer was loaded with was calculated by multiplying the product of concentration of ACh in the loading solution used and the volume used ($[ACh]*L_s$) by the molecular weight of acetylcholine (146.2g/mol, Equation 3). The amount of ACh from each assay sample was then calculated using the log of the integrated area of the sample ($Log(IA_i)$ to solve for the point slope equation of the calibration curve (b= 9.0269, x=0.3814, Equation 4). The mass of ACh recovered from each treatment was calculated by raising 10 to the power of the solution of the corresponding iteration of equation 4 ($log[ACh]_i$) then multiplying it by the volume (L_i) and molecular weight of ACh (146.2g/mol) and the corresponding volume of the sample the calculated percent of ACh recovered from a particular treatment or overall was then simply divided by the calculated amount of ACh a polymer was loaded with.

Equation 3 – Calculation of Mass of Loaded Acetylcholine

$([ACh]*L_s)*(146.2g/mole) = g_{ACh}$

Equation 4 – Calculation of Concentration of Acetylcholine Recovered

$(Log(IA_i) – 9.0269/0.3814) = log([ACh]_i)$

Equation 5 – Calculation of Mass of Acetylcholine Recovered

$(10^{(log([ACh]_i)) * L_i * 146.2g/mole = g_{ACh}}$

Results

Figure 3 – A Visual Representation of AutoDock Analysis of Acetylcholine Interactions with Active Site Amino Acid Residues of Acetylcholinesterase

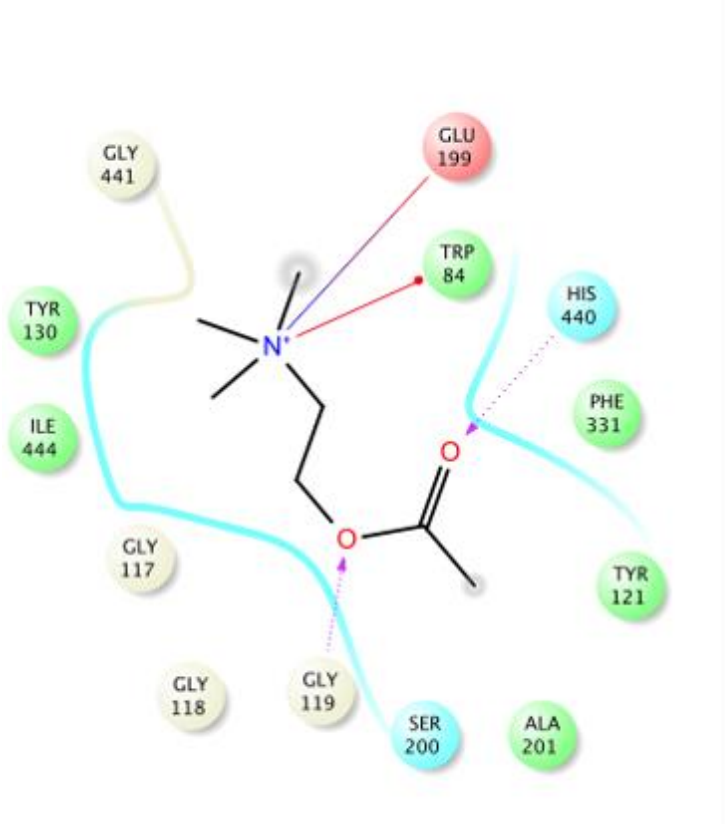

Figure 3 - A visual representation of the most favorable site for acetylcholine (ACH)-acetylcholinesterase (AChE) interaction, according to the docking study performed with AutoDock. This site was further analyzed using the visualization software called Maestro, which allowed for a clean representation of the site and the interactions that facilitate the ligand-protein interaction. The purple arrows extending from glycine 119 (Gly^{119}) and histidine (His^{440}) represent hydrogen bond interactions. The red line extending from tryptophan (Trp^{84}) represents a pi-cation interaction. Lastly, the red and blue line connecting glutamate (Glu^{199}) and ACh represents an ionic interaction. Sussman et al. reported that His^{440} was a part of the active site of ACh sterase, and that Gly^{119} was integral in guiding ACh into said active site (Sussman, 1991).

Table 1 – Calculated Stabilization Energies of acetylcholine-functional monomer Complexes Analyzed with GAMESS

Functional monomer (FM)	ΔE 1ACh:1FM (kJ/mol)	ΔE 1ACh:2FM (kJ/mol)	ΔE 1ACh:3FM (kJ/mol)
Methacrylic acid	-34.54	-101.82	-152.04
Acrylic acid	-76.34	-124	-177.17
Methacrylamide	-61.24	-130.82	-163.11
Acrylamide	-92.4	-150.77	-175.72
Itaconic Acid	-85.66	-180.44	-197.51

*Table 1- The stabilization energy for each complex that was screened is displayed in table 8. Each Functional monomer was placed into a complex with ACh at a ratio of 1:1, 1:2, and 1:3. Density Functional Theory (B3LYP, 6-31G(d,p), gas phase) was then used in order to calculate the equilibrium geometry, or in other words the lowest total energy, for each complex. The stabilization energy for each complex was then calculated using the total energy of the complex and its respective compounds in equation 1 (ΔE = E(template - monomer) – {E(template) + ΣE(monomer)}). The calculated stabilization energy for each complex was then converted from atomic units (a.u.) to kilojoules per mole (kJ/mol) using equation 2 (ΔE * 1 a.u). * {(627.51 kcal/mol) / (1 a.u)} * {(4.184 kJ/mol) / (1 kcal/mol)} = (ΔE* 2625.50 kJ/mol). ACh -itaconic acid (1ACh:X IA, where X= an integer value 1, 2, or 3) complexes had the lowest overall stabilization energy (ΔE 1 ACh:3 IA= -197.51kJ/mol), and the lowest stabilization energy among 1 ACh:2 functional monomer complexes (ΔE 1ACh:2 IA= -180.44kJ/mol). Acrylamide formed the lowest stabilization energy among 1:1 complexes (ΔE 1ACh:1 A= -92.40 kJ/mol).*

Figure 4 – Log Log Linear Calibration Curve of Acetylcholine Standard Solutions

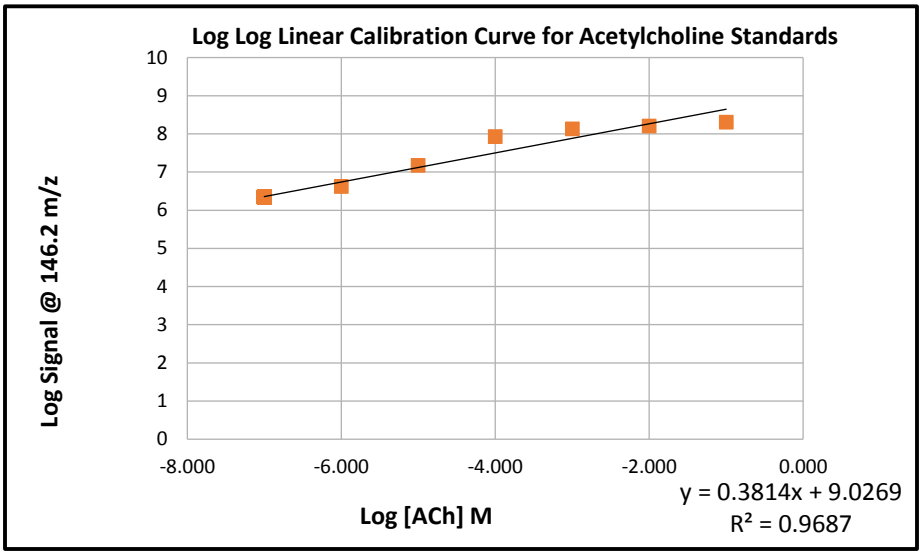

Figure 4 - A series of standards with a known concentration of ACh ranging from 100mM to 100nM were sampled to collect data for a calibration curve via FIA-MS analysis. Injections were made with volumes of 20µL, a flow rate of 0.1mL/min, 20% MeOH mobile phase, and no external heat source. The log of the signal generated in Single ion extraction mode at 146.2 m/z was plotted against the log of ACh concentration. The integration of the area under the signal at 146.2 m/z in Q1 for each standard was then taken from 0.2 to 1.2min. The linear regression analysis of the scatterplot provided a point slope equation, that was used to approximate the concentration of ACh in unknown samples collected from the binding capacity assay.

Figure 5.1- Binding Assay Results from SDS/AcOH Elution Solution

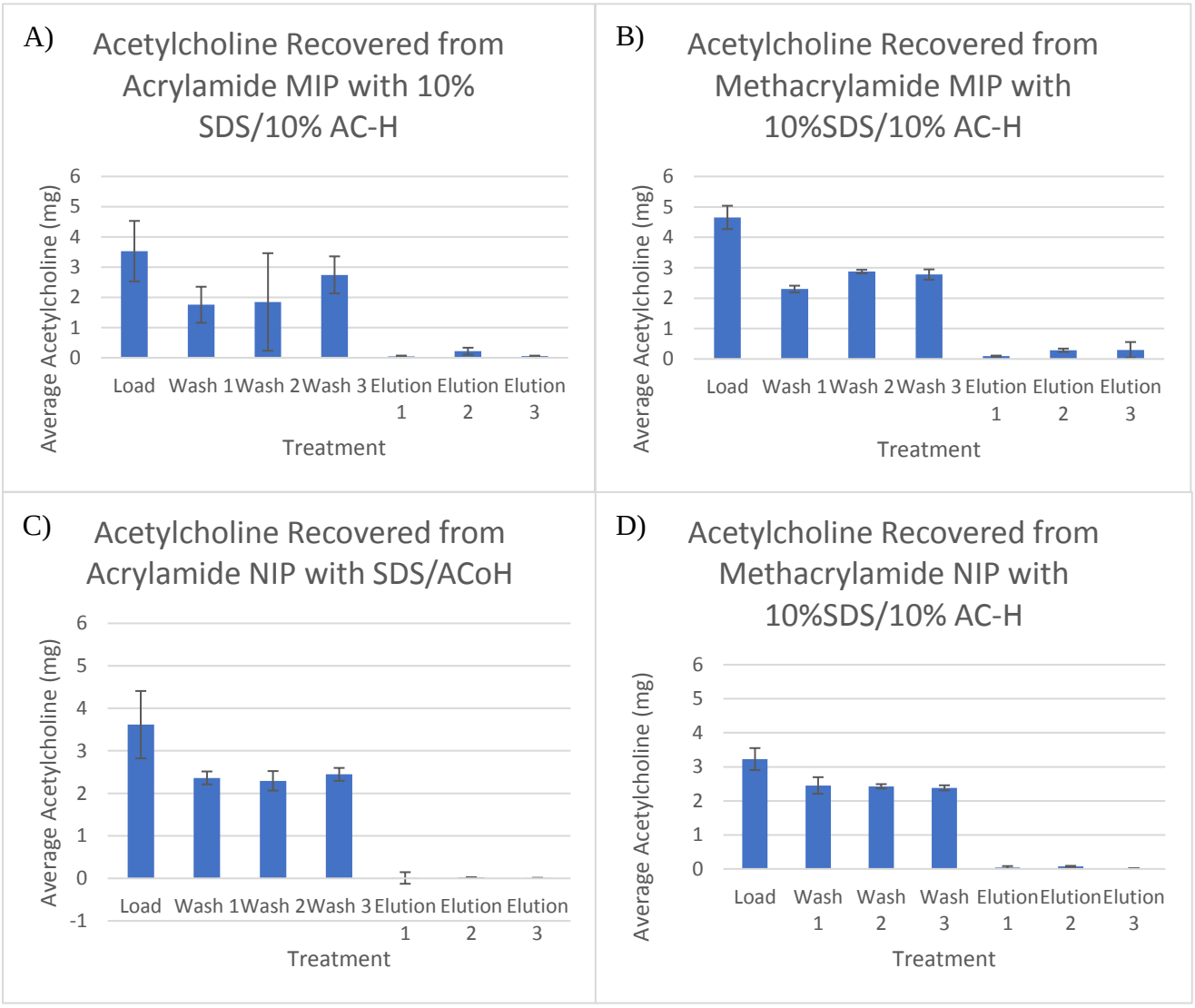

Figure 5.1 - the average ACh collected (y-axis) from each different treatment (x-axis) is shown for each group of polymers (A, B, C, & D; n=3 per group) treated with the SDS/AcOH elution solution. The "Load" treatment was an 80mM ACh stock solution, which was added during synthesis for experimental MIPs and after synthesis for 20 minutes on a stir rack for control NIPs. Experimental MIPs were loaded with 48mg ACh (A & B), while all control polymers were loaded with 36mg ACh (C & D). All "Wash" treatments consisted solely of DIH_2O, which was applied for 20 minutes on a stir rack for all polymers. The "Elution" treatment for this group was the 10%SDS/10%AcOH in DIH_2O elution solution, which was also applied for 20 minutes on a stir rack. The volume of the control "Load" treatments for this elution solution was 3mL, but the rest of the treatments were applied in 2mL volumes. Each treatment was collected after application for 20 minutes, then subjected to FIA-MS analysis. FIA-MS analysis was carried out in 20 µL injection volumes with 20% meOH mobile phase at 0.1mL/min with no external heating source. The integration of the area under the signal at 146.2 m/z in Q1 for each sample was then taken from 0.2 to 1.2min. The log of the integrated area for each sample was then used with the point slope equation from the calibration curve to calculate its estimated concentration of ACh (Equations 3 & 4).

Figure 5.2– Binding Assay Results from MeOH/AcOH Elution Solution

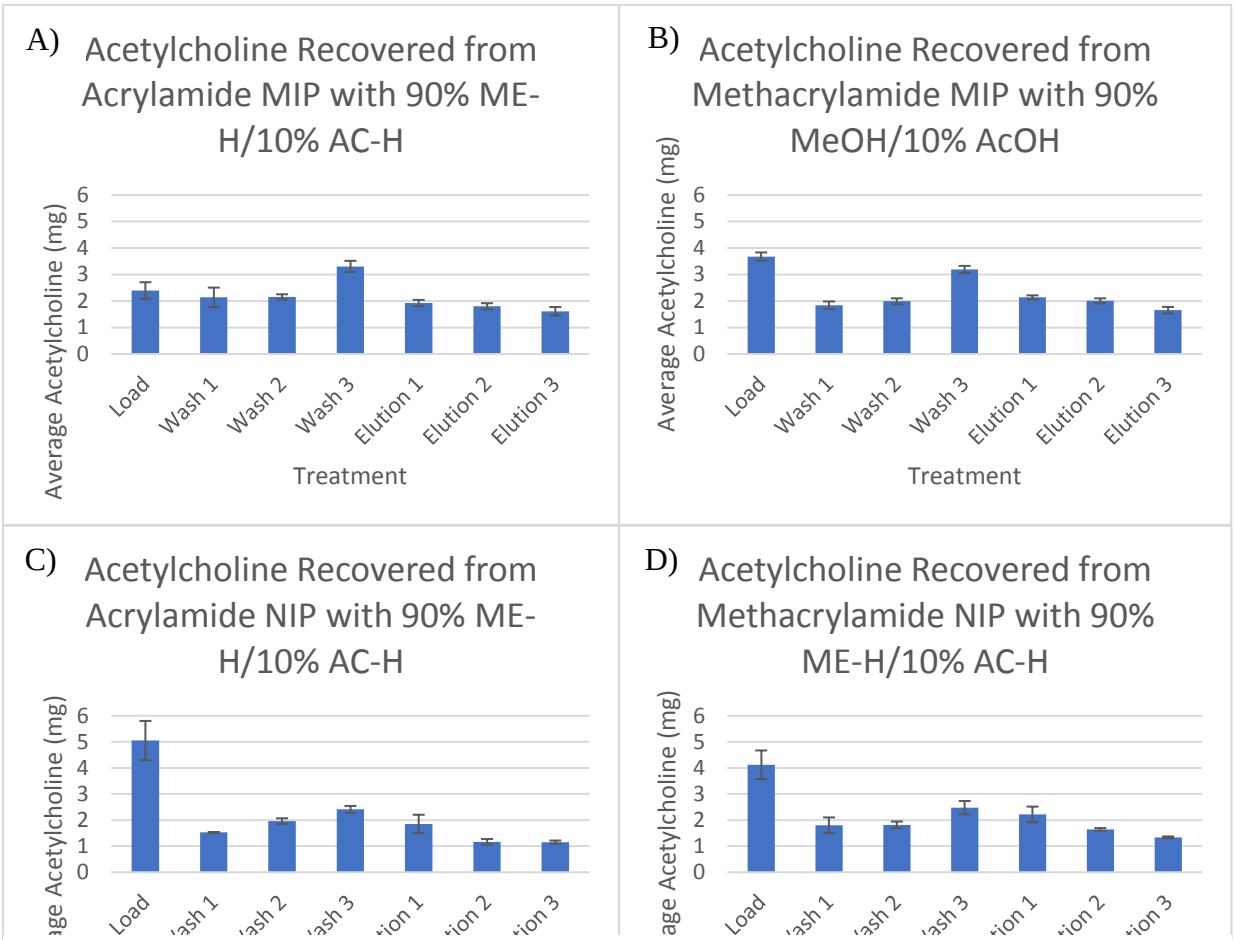

Figure 5.2 - The average ACh collected (y-axis) from each different treatment (x-axis) is shown for each group of polymers (A, B, C, & D; n=3 per group) treated with the MeOH/AcOH elution solution. The "Load" treatment was an 80mM ACh stock solution, which was added during synthesis for experimental MIPs and after synthesis for 20 minutes on a stir rack for control NIPs. Experimental MIPs were loaded with 48mg ACh (A & B), while all control polymers were loaded with 36mg ACh (C & D). All "Wash" treatments consisted solely of DIH_2O, which was applied for 20 minutes on a stir rack for all polymers. The "Elution" treatment for this group was the 90%MeOH/10%AcOH elution solution, which was also applied for 20 minutes on a stir rack. The volume of the control "Load" treatments for this elution solution was 3mL (C & D), but the rest of the treatments were applied in 2mL volumes (A & B). Each treatment was collected after application for 20 minutes, then subjected to FIA-MS analysis. FIA-MS analysis was carried out in 20 µL injection volumes with 20% meOH mobile phase at 0.1mL/min with no external heating source. The integration of the area under the signal at 146.2 m/z in Q1 for each sample was then taken from 0.2 to 1.2min. The log of the integrated area for each sample was then used with the point slope equation from the calibration curve to calculate the estimated amount of ACh recovered in each assay sample. The average of the estimated ACh concentration was then used to calculate the average amount of ACh retrieved from each treatment (Equations 3 & 4).

Figure 5.3– Binding Assay Results from KCl Elution Solution

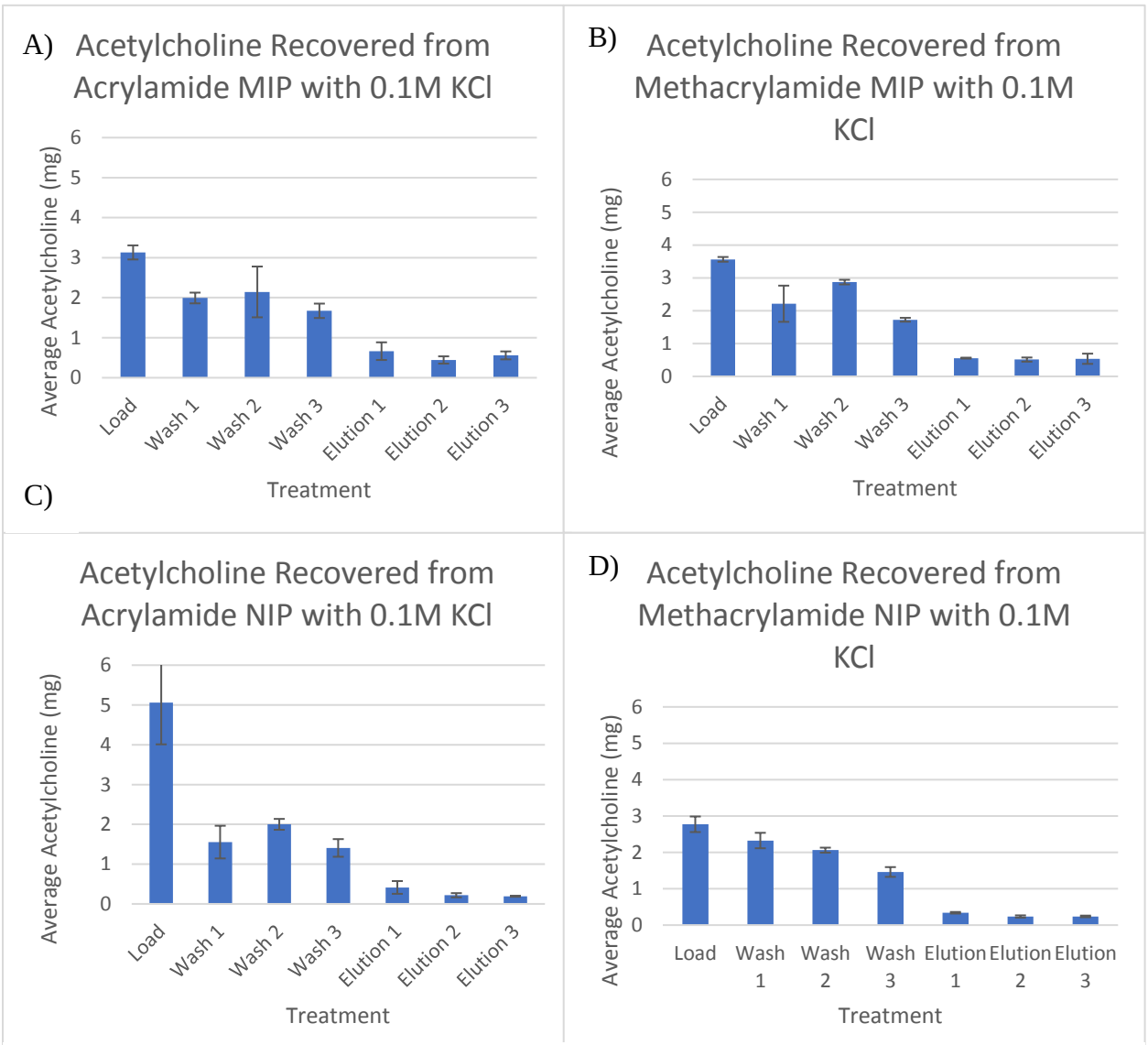

Figure 5.3 – The average ACh collected (y-axis) from each different treatment (x-axis) is shown for each group of polymers (A, B, C, & D; n=3 per group) treated with the KCl elution solution. The "Load" treatment was an 80mM ACh stock solution, which was added during synthesis for experimental MIPs and after synthesis for 20 minutes on a stir rack for control NIPs. Experimental MIPs were loaded with 48mg ACh (A & B), while all control polymers were loaded with 24mg ACh (C & D). All "Wash" treatments consisted solely of DIH_2O, which was applied for 20 minutes on a stir rack for all polymers. The "Elution" treatment for this group was the 0.1M KCl elution solution, which was also applied for 20 minutes on a stir rack. All the treatments in this elution solution were applied in 2mL volumes. Each treatment was collected after application for 20 minutes, then subjected to FIA-MS analysis. FIA-MS analysis was carried out in 20 µL injection volumes with 20% meOH mobile phase at 0.1mL/min with no external heating source. The integration of the area under the signal at 146.2 m/z in Q1 for each sample was then taken from 0.2 to 1.2min. The log of the integrated area for each sample was then used with the point slope equation from the calibration curve to calculate its estimated concentration of ACh(reference to sample math in materials?). The average of the estimated ACh concentration was then used to calculate the average amount of ACh retrieved from each treatment (Equations 3 & 4).

Figure 5.4– Binding Assay Results from Tris-HCl Elution Solution

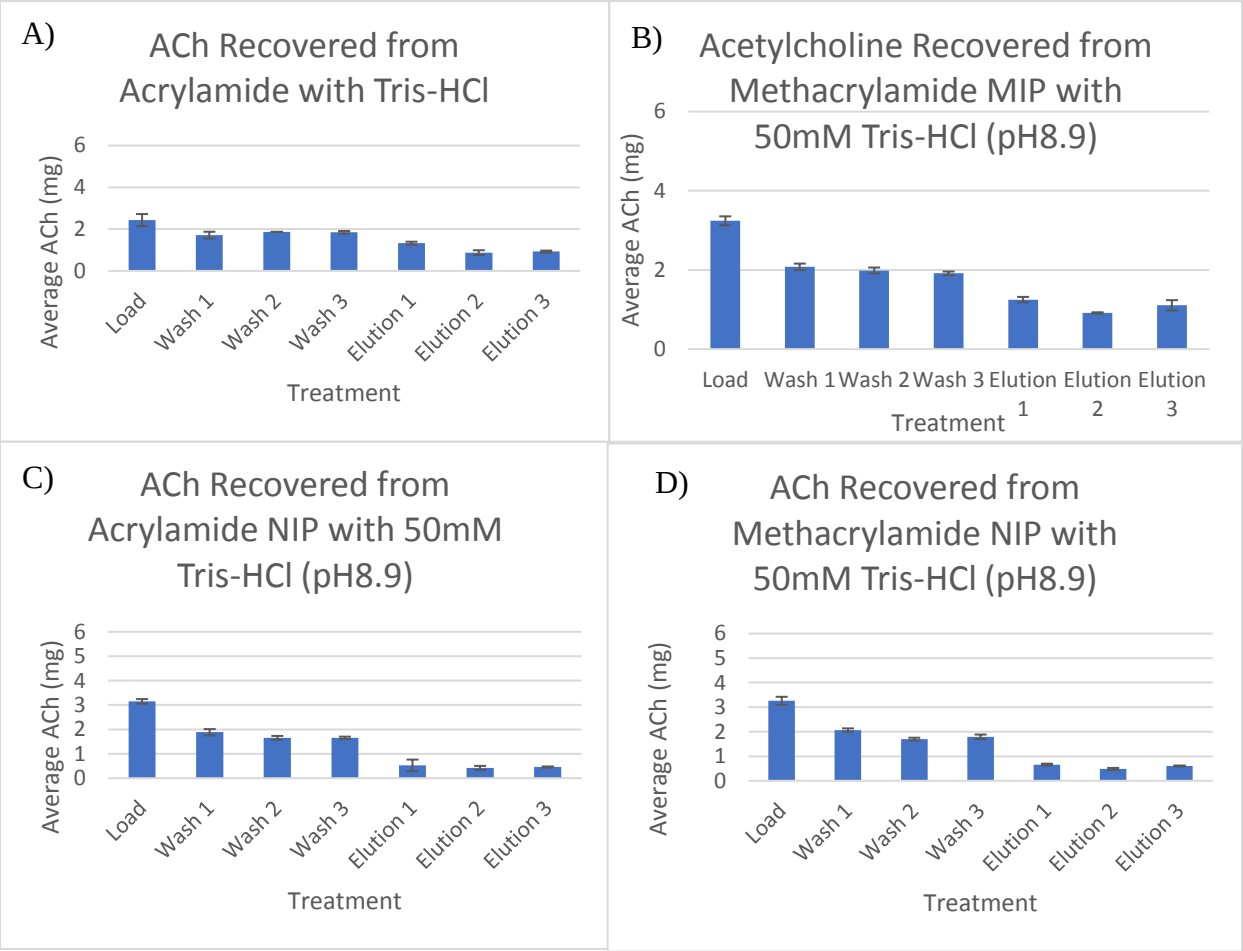

Figure 5.4 - he average ACh collected (y-axis) from each different treatment (x-axis) is shown for each group of polymers (A, B, C, & D; n=3 per group) treated with the SDS/AcOH elution solution. The "Load" treatment was an 80mM ACh stock solution, which was added during synthesis for experimental MIPs and after synthesis for 20 minutes on a stir rack for control NIPs. Experimental MIPs were loaded with 48mg ACh (A & B), while all control polymers were loaded with 24mg ACh (C & D). All "Wash" treatments consisted solely of DIH_2O, which was applied for 20 minutes on a stir rack for all polymers. The "Elution" treatment for this group was the 50mM Tris Tris-HCl solution (pH8.9) KCl elution solution, which was also applied for 20 minutes on a stir rack. All the treatments in this elution solution were applied in 2mL volumes. Each treatment was collected after application for 20 minutes, then subjected to FIA-MS analysis. FIA-MS analysis was carried out in 20 µL injection volumes with 20% meOH mobile phase at 0.1mL/min with no external heating source. The integration of the area under the signal at 146.2 m/z in Q1 for each sample was then taken from 0.2 to 1.2min. The log of the integrated area for each sample was then used with the point slope equation from the calibration curve to calculate its estimated concentration of ACh(reference to sample math in materials and methods?). The average of the estimated ACh concentration was then used to calculate the average amount of ACh retrieved from each treatment (Equations 3 & 4).

Figure 6 – Calculated Percent of Acetylcholine Recovered from Each Elution Solution

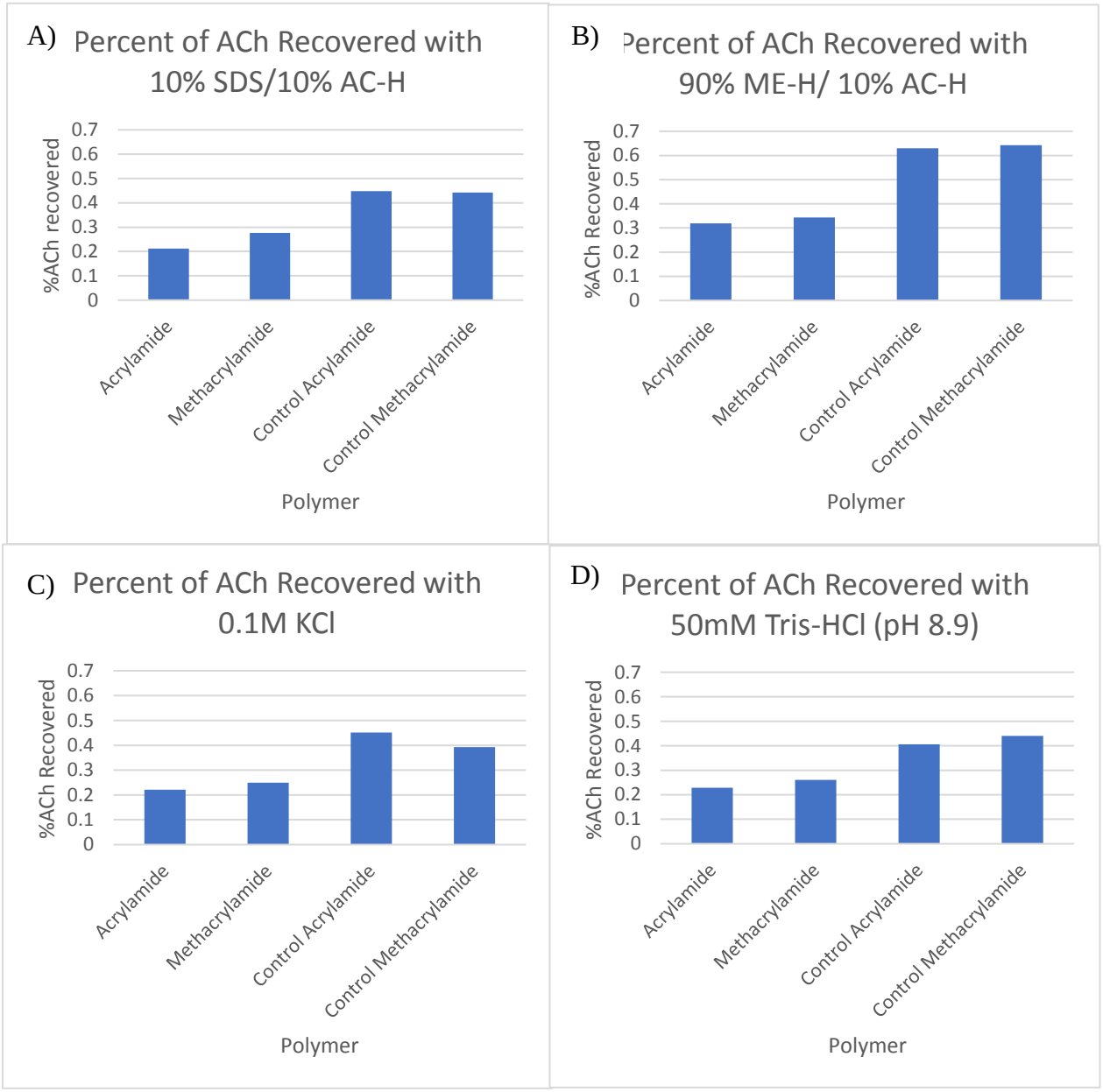

Figure 6 - A side by side comparison of how the four different kinds of polymers faired across each different elution solution in terms of percent of ACh recovered in total. The average amount of ACh recovered across all treatments was added up and then divided by the original amount of ACh that it was originally loaded with. The values of ACh originally added were 24, 36, and 48mg for control NIPs, control NIPs from the SDS/AcOH elution solution as well as the MeOH/AcOH elution solution, and the experimental MIPs, respectively

Discussion

The object of this experiment was to synthesize functional ACh imprinted polymers, that could potentially be used as alternative recognition elements in ACh biosensors. AChE, a protein that is frequently used in contemporary ACh biosensors, was studied order to discern what electrochemical forces drove its interaction with ACh. Analysis with the docking software, Autodock, revealed AChE interaction with ACh is primarily driven by hydrogen bonding, ionic interactions, and dispersion forces (Visualized with Maestro in Figure). The pi-cation binding (seen between ACh and Trp^{84} in figure 1) is a type of dispersion force, which is particularly generated by a large electron cloud. it was decided that an attempt to recapitulate this pi-cation interaction should not be made, due to the inability to model such large electron systems. Instead, it was thought that GAMESS would have an easier time calculating the equilibrium geometry of smaller electron systems that did not feature large pi orbitals as seen in phenyl groups and other conjugated ring structures.

As indicated, the quantum calculator, GAMESS, was used to calculate what functional monomers out of methacrylic acid, acrylic acid, itaconic acid, acrylamide, and methacrylamide formed the most energetically favorable complex in gaseous phase (Figure). Of these functional monomers, itaconic acid, acrylamide, and methacrylamide appeared to present the most potential for forming a complex with ACh *in vitro* (Table Y). Syntheses that were subsequently attempted using a protocol proposed by the Hawkins group only yielded polymers when using the functional monomers acrylamide and methacrylamide (Hawkins, 2016). Despite the high theoretical favorability to form a complex with ACh, it seemed that the mechanism in the Hawkins synthesis required an amide group for matrix formation, which itaconic did not feature.

There is a strong precedent for using log vs log relationships in FIA-MS analysis (Milardović, 1997; Fang, 2000). A calibration curve was made (Figure X) using the integrated area of the MS signal at 146.2 m/z. The average amount of ACh recovered from each treatment was calculated using the point slope equation (Figures WXYZ). The overall percent of ACh recovered from the binding Assay was then calculated using the calculated amount recovered and the known amount of ACh added (Figure X). In general, the experimental MIPs displayed a much lower rate of ACh recovery than the control NIPs. This indicated that the experimental MIP could potentially have been imprinted for actylcholine, although more work is needed to completely verify this. The best method for template elution seems to be the 90% MeOH/10% AcOH mixture. However, it was qualitatively corrosive to the MIPs and NIPs, therefore it would be best to dilute the MeOH in the future to prevent unwanted breakdown of the polymer matrix. Overall, there is a significant potential for proof of concept in results of gathered. However, further work is needed to refine the quantitative and acquisition methods in FIA-MS analysis in order to properly quantitate results in any future work. The calibration curve specifically can use major improvements, as well as overall aspects of the binding assay procedure. The potential successful imprinting of polymers for ACh highlights the progress made in technology, and offers precedence for other groups lacking funding to take a similar approach in their projects. Future works seeking to carry o this research should try to molecularly sieve the polymers, because it was original part of the Hawkin's synthesis (Hawkins, 2004). Alternatively it could be worthwhile to run another binding capacity in a container with small height, but large length and width to maximize surface area and treatment interaction.

Works Cited

Ahmadi, F., Ahmadi, J., & Rahimi-Nasrabadi, M. (2011). Computational approaches to design a molecular imprinted polymer for high selective extraction of 3,4-methylenedioxymethamphetamine from plasma. *Journal of Chromatography. A*, *1218*(43), 7739–7747. https://doi.org/10.1016/j.chroma.2011.08.020

Alexander, C., Andersson, H. S., Andersson, L. I., Ansell, R. J., Kirsch, N., Nicholls, I. A., … Whitcombe, M. J. (2006). Molecular imprinting science and technology: a survey of the literature for the years up to and including 2003. *Journal of Molecular Recognition*, *19*(2), 106–180. https://doi.org/10.1002/jmr.760

Costa, L. G., Cole, T. B., Coburn, J., Chang, Y.-C., Dao, K., & Roque, P. (2014). Neurotoxicants Are in the Air: Convergence of Human, Animal, and In Vitro Studies on the Effects of Air Pollution on the Brain [Research article]. https://doi.org/10.1155/2014/736385

Diñeiro, Y., Menéndez, M. I., Blanco-López, M. C., Lobo-Castañón, M. J., Miranda-Ordieres, A. J., & Tuñón-Blanco, P. (2006). Computational predictions and experimental affinity distributions for a homovanillic acid molecularly imprinted polymer. *Biosensors and Bioelectronics*, *22*(3), 364–371. https://doi.org/10.1016/j.bios.2006.03.027

Dunphy, R., & Burinsky, D. J. (2003). Detection of choline and acetylcholine in a pharmaceutical preparation using high-performance liquid chromatography/electrospray ionization mass spectrometry. *Journal of Pharmaceutical and Biomedical Analysis*, *31*(5), 905–915. https://doi.org/10.1016/S0731-7085(02)00674-X

Fang, L., Wan, M., Pennacchio, M., & Pan, J. (2000). Evaluation of Evaporative Light-Scattering Detector for Combinatorial Library Quantitation by Reversed Phase HPLC. *Journal of Combinatorial Chemistry*, *2*(3), 254–257. https://doi.org/10.1021/cc990068e

Foster, M. E., & Sohlberg, K. (2009). Empirically corrected DFT and semi-empirical methods for non-bonding interactions. *Physical Chemistry Chemical Physics*, *12*(2), 307–322. https://doi.org/10.1039/B912859J

Giniatullin, R., Nistri, A., & Yakel, J. L. (2005). Desensitization of nicotinic ACh receptors: shaping cholinergic signaling. *Trends in Neurosciences*, *28*(7), 371–378. https://doi.org/10.1016/j.tins.2005.04.009

Guan, H., Zhang, F., Yu, J., & Chi, D. (2012). The novel acetylcholinesterase biosensors based on liposome bioreactors–chitosan nanocomposite film for detection of organophosphates pesticides. *Food Research International*, *49*(1), 15–21. https://doi.org/10.1016/j.foodres.2012.07.014

Hadizadeh, F., Hassanpour Moghadam, M., & Mohajeri, S. A. (2013). Application of molecularly imprinted hydrogel for the preparation of lactose-free milk. *Journal of the Science of Food and Agriculture*, *93*(2), 304–309. https://doi.org/10.1002/jsfa.5757

Hawkins, D. M., Stevenson, D., & Reddy, S. M. (2005). Investigation of protein imprinting in hydrogel-based molecularly imprinted polymers (HydroMIPs). *Analytica Chimica Acta*, *542*(1), 61–65. https://doi.org/10.1016/j.aca.2005.01.052

Hawkins, D. M., Trache, A., Ellis, E. A., Stevenson, D., Holzenburg, A., Meininger, G. A., & Reddy, S. M. (2006). Quantification and Confocal Imaging of Protein Specific Molecularly Imprinted Polymers. *Biomacromolecules*, *7*(9), 2560–2564. https://doi.org/10.1021/bm060494d

Jarrett, P., Easton, A., Rockwood, K., Dyack, S., McCollum, A., Siu, V., … Darvesh, S. (2018). Evidence for Cholinergic Dysfunction in Autosomal Dominant Kufs Disease. *Canadian Journal of Neurological Sciences*, *45*(2), 150–157. https://doi.org/10.1017/cjn.2017.261

Khairi, N. A. S., Yusof, N. A., Abdullah, A. H., & Mohammad, F. (2015). Removal of Toxic Mercury from Petroleum Oil by Newly Synthesized Molecularly-Imprinted Polymer. *International Journal of Molecular Sciences*, *16*(5), 10562–10577. https://doi.org/10.3390/ijms160510562

Khan, A., Khan, A. A. P., Asiri, A. M., Rub, M. A., Azum, N., Rahman, M. M., … Ghani, S. A. (2013). A New Trend on Biosensor for Neurotransmitter Choline/Acetylcholine—an Overview. *Applied Biochemistry and Biotechnology*, *169*(6), 1927–1939. https://doi.org/10.1007/s12010-013-0099-0

Khimji, I., Kelly, E. Y., Helwa, Y., Hoang, M., & Liu, J. (2013). Visual optical biosensors based on DNA-functionalized polyacrylamide hydrogels. *Methods*, *64*(3), 292–298. https://doi.org/10.1016/j.ymeth.2013.08.021

Kim, H. G., Moon, M., Choi, J. G., Park, G., Kim, A.-J., Hur, J., … Oh, M. S. (2014). Donepezil inhibits the amyloid-beta oligomer-induced microglial activation in vitro and in vivo. *NeuroToxicology*, *40*, 23–32. https://doi.org/10.1016/j.neuro.2013.10.004

Kimura, Y., Sato, N., Ota, M., Maikusa, N., Maekawa, T., Sone, D., … Sugimoto, H. (2017). A structural MRI study of cholinergic pathways and cognition in multiple sclerosis. *ENeurologicalSci*, *8*, 11–16. https://doi.org/10.1016/j.ensci.2017.06.008

Lin Ding, D. D. (2008). Trends in Cell-Based Electrochemical Biosensors. *Current Medicinal Chemistry*, *15*(30), 3160–3170. https://doi.org/10.2174/092986708786848514

Milardović, S., Kruhak, I., Iveković, D., Rumenjak, V., Tkalčec, M., & Grabarić, B. S. (1997). Glucose determination in blood samples using flow injection analysis and an amperometric biosensor based on glucose oxidase immobilized on hexacyanoferrate modified nickel electrode. *Analytica Chimica Acta*, *350*(1), 91–96. https://doi.org/10.1016/S0003-2670(97)00308-5

Nakamura, H., & Karube, I. (2003). Current research activity in biosensors. *Analytical and Bioanalytical Chemistry*, *377*(3), 446–468. https://doi.org/10.1007/s00216-003-1947-5

Nanita, S. C., & Kaldon, L. G. (2016). Emerging flow injection mass spectrometry methods for high-throughput quantitative analysis. *Analytical and Bioanalytical Chemistry*, *408*(1), 23–33. https://doi.org/10.1007/s00216-015-9193-1

Nicholls, I. A., Andersson, H. S., Golker, K., Henschel, H., Karlsson, B. C. G., Olsson, G. D., … Wikman, S. (2011). Rational design of biomimetic molecularly imprinted materials: theoretical and computational strategies for guiding nanoscale structured polymer development. *Analytical and Bioanalytical Chemistry*, *400*(6), 1771–1786. https://doi.org/10.1007/s00216-011-4935-1

Nirogi, R., Mudigonda, K., Kandikere, V., & Ponnamaneni, R. (2010). Quantification of acetylcholine, an essential neurotransmitter, in brain microdialysis samples by liquid chromatography mass spectrometry. *Biomedical Chromatography*, *24*(1), 39–48. https://doi.org/10.1002/bmc.1347

Pavel, D., & Lagowski, J. (2005). Computationally designed monomers and polymers for molecular imprinting of theophylline and its derivatives. Part I. *Polymer*, *46*(18), 7528–7542. https://doi.org/10.1016/j.polymer.2005.04.099

Perry, M., Li, Q., & Kennedy, R. T. (2009). Review of recent advances in analytical techniques for the determination of neurotransmitters. *Analytica Chimica Acta*, *653*(1), 1–22. https://doi.org/10.1016/j.aca.2009.08.038

Philip, N. S., Carpenter, L. L., Tyrka, A. R., & Price, L. H. (2010). Nicotinic acetylcholine receptors and depression: a review of the preclinical and clinical literature. *Psychopharmacology*, *212*(1), 1–12. https://doi.org/10.1007/s00213-010-1932-6

Saridakis, E., Khurshid, S., Govada, L., Phan, Q., Hawkins, D., Crichlow, G. V., … Chayen, N. E. (2011). Protein crystallization facilitated by molecularly imprinted polymers- Supplemental Information. *Proceedings of the National Academy of Sciences*, *108*(27), 11081–11086. https://doi.org/10.1073/pnas.1016539108

Saridakis, Emmanuel, Khurshid, S., Govada, L., Phan, Q., Hawkins, D., Crichlow, G. V., … Chayen, N. E. (2011). Protein crystallization facilitated by molecularly imprinted polymers. *Proceedings of the National Academy of Sciences*, *108*(27), 11081–11086. https://doi.org/10.1073/pnas.1016539108

Shoravi, S., Olsson, G. D., Karlsson, B. C. G., & Nicholls, I. A. (2014). On the Influence of Crosslinker on Template Complexation in Molecularly Imprinted Polymers: A Computational Study of Prepolymerization Mixture Events with Correlations to Template-Polymer Recognition Behavior and NMR Spectroscopic Studies. *International Journal of Molecular Sciences*, *15*(6), 10622–10634. https://doi.org/10.3390/ijms150610622

Soreq, H. (2015). Checks and balances on cholinergic signaling in brain and body function. *Trends in Neurosciences*, *38*(7), 448–458. https://doi.org/10.1016/j.tins.2015.05.007

Suriyo, T., Tachachartvanich, P., Visitnonthachai, D., Watcharasit, P., & Satayavivad, J. (2015). Chlorpyrifos promotes colorectal adenocarcinoma H508 cell growth through the activation of EGFR/ERK1/2 signaling pathway but not cholinergic pathway. *Toxicology*, *338*, 117–129. https://doi.org/10.1016/j.tox.2015.10.009

Tansey, E. M. (2006). Henry Dale and the discovery of acetylcholine. *Comptes Rendus Biologies*, *329*(5–6), 419–425. https://doi.org/10.1016/j.crvi.2006.03.012

V. Uteshev, V. (2016, April). Editorial (Thematic Issue: Effective and Promising Treatments for Neurological Disorders and Cancer) [Text]. Retrieved May 9, 2018, from http://www.ingentaconnect.com.ezproxy.trincoll.edu/contentone/ben/cpd/2016/00000022/00000014/art00001

Wach, A., Chen, J., Falls, Z., Lonie, D., Mojica, E.-R., Aga, D., … Zurek, E. (2013). Determination of the Structures of Molecularly Imprinted Polymers and Xerogels Using an Automated Stochastic Approach. *Analytical Chemistry*, *85*(18), 8577–8584. https://doi.org/10.1021/ac402004z

Woolf, N. J., & Butcher, L. L. (2011). Cholinergic systems mediate action from movement to higher consciousness. *Behavioural Brain Research*, *221*(2), 488–498. https://doi.org/10.1016/j.bbr.2009.12.046

Young, D. C. (2001). Density Functional Theory. In *Computational Chemistry* (pp. 42–48). John Wiley & Sons, Inc. https://doi.org/10.1002/0471220655.ch5

Zackheim, J. A., & Abercrombie, E. D. (2003). HPLC/EC Detection and Quantification of Acetylcholine in Dialysates. In *Drugs of Abuse* (pp. 433–441). Humana Press. https://doi.org/10.1385/1-59259-358-5:433

Appendix

Raw Data from SDS/AcOH Elution Solution Group

Sample	gel type	Wash Type	area	Volume	ACh (mg)
1	A	L	2.199E+08	0.002	4.685256
2	A	L	1.840E+08	0.002	2.938687
3	A	L	1.846E+08	0.002	2.961965
4	MA	L	2.271E+08	0.002	5.096542
5	MA	L	2.147E+08	0.002	4.399809
6	MA	L	2.160E+08	0.002	4.469684
7	CA	L	1.835E+08	0.003	4.375513
8	CA	L	1.718E+08	0.003	3.677337
9	CA	L	1.547E+08	0.003	2.79474
10	CMA	L	1.659E+08	0.003	3.358497
11	CMA	L	1.561E+08	0.003	2.861808
12	CMA	L	1.679E+08	0.003	3.465434
13	A	W1	1.250E+08	0.002	1.066248
14	A	W1	1.626E+08	0.002	2.125278
15	A	W1	1.611E+08	0.002	2.073008
16	MA	W1	1.661E+08	0.002	2.245542
17	MA	W1	1.657E+08	0.002	2.23139
18	MA	W1	1.711E+08	0.002	2.426953
19	CA	W1	1.648E+08	0.002	2.198946
20	CA	W1	1.702E+08	0.002	2.393048
21	CA	W1	1.730E+08	0.002	2.498196
22	CMA	W1	1.722E+08	0.002	2.468317
23	CMA	W1	1.649E+08	0.002	2.201691
24	CMA	W1	1.779E+08	0.002	2.687816
25	A	W2	1.742E+08	0.002	2.545176
26	A	W2	8.530E+06	0.002	0.000934
27	A	W2	1.854E+08	0.002	2.995983
28	MA	W2	1.831E+08	0.002	2.899088
29	MA	W2	1.835E+08	0.002	2.916462
30	MA	W2	1.808E+08	0.002	2.805084
31	CA	W2	1.671E+08	0.002	2.280322
32	CA	W2	1.739E+08	0.002	2.531468
33	CA	W2	1.612E+08	0.002	2.07487

34	CMA	W2	1.730E+08	0.002	2.499528
35	CMA	W2	1.705E+08	0.002	2.405192
36	CMA	W2	1.698E+08	0.002	2.377815
37	A	W3	1.744E+08	0.002	2.552734
38	A	W3	1.952E+08	0.002	3.429323
39	A	W3	1.662E+08	0.002	2.248797
40	MA	W3	1.806E+08	0.002	2.796633
41	MA	W3	1.756E+08	0.002	2.598963
42	MA	W3	1.840E+08	0.002	2.935208
43	CA	W3	1.671E+08	0.002	2.279467
44	CA	W3	1.726E+08	0.002	2.483939
45	CA	W3	1.750E+08	0.002	2.575873
46	CMA	W3	1.689E+08	0.002	2.346324
47	CMA	W3	1.686E+08	0.002	2.335452
48	CMA	W3	1.722E+08	0.002	2.469597
49	A	E1	2.889E+07	0.002	0.022893
50	A	E1	4.580E+07	0.002	0.076624
51	A	E1	3.257E+07	0.002	0.031346
52	MA	E1	4.459E+07	0.002	0.071421
53	MA	E1	5.060E+07	0.002	0.09951
54	MA	E1	5.184E+07	0.002	0.106001
55	CA	E1	1.732E+07	0.002	0.005986
56	CA	E1	2.195E+07	0.002	0.011137
57	CA	E1	2.181E+07	0.002	0.010954
58	CMA	E1	4.895E+07	0.002	0.091225
59	CMA	E1	2.794E+07	0.002	0.02097
60	CMA	E1	2.751E+07	0.002	0.020132
61	A	E2	5.790E+07	0.002	0.141682
62	A	E2	8.179E+07	0.002	0.350488
63	A	E2	6.026E+07	0.002	0.157307
64	MA	E2	7.100E+07	0.002	0.241821
65	MA	E2	7.408E+07	0.002	0.270356
66	MA	E2	8.147E+07	0.002	0.346886
67	CA	E2	2.497E+07	0.002	0.015615
68	CA	E2	2.731E+07	0.002	0.019748
69	CA	E2	3.144E+07	0.002	0.028568
70	CMA	E2	4.917E+07	0.002	0.092316
71	CMA	E2	4.488E+07	0.002	0.072668
72	CMA	E2	4.090E+07	0.002	0.056954
73	A	E3	3.574E+07	0.002	0.039985
74	A	E3	4.404E+07	0.002	0.06913
75	A	E3	4.071E+07	0.002	0.056248
76	MA	E3	6.135E+07	0.002	0.16489
77	MA	E3	5.742E+07	0.002	0.138626

78	MA	E3	1.002E+08	0.002	0.59628
79	CA	E3	2.124E+07	0.002	0.010217
80	CA	E3	1.972E+07	0.002	0.008407
81	CA	E3	2.129E+07	0.002	0.010277
82	CMA	E3	2.170E+07	0.002	0.010803
83	CMA	E3	2.676E+07	0.002	0.018727
84	CMA	E3	2.913E+07	0.002	0.023398

Raw Data from MeOH:AcOH Elution Solution

Sample	gel type	Wash Type	Area	volume	ACh (mg)
1	A	L	1.790E+08	0.002	2.730909
2	A	L	1.624E+08	0.002	2.115133
3	A	L	1.690E+08	0.002	2.349983
4	MA	L	2.005E+08	0.002	3.677491
5	MA	L	1.973E+08	0.002	3.526741
6	MA	L	2.037E+08	0.002	3.833445
7	CA	L	2.050E+08	0.003	5.846525
8	CA	L	1.925E+08	0.003	4.956989
9	CA	L	1.831E+08	0.003	4.348327
10	CMA	L	1.894E+08	0.003	4.753906
11	CMA	L	1.749E+08	0.003	3.855309
12	CMA	L	1.732E+08	0.003	3.760491
13	A	W1	1.493E+08	0.003	2.546686
14	A	W1	1.537E+08	0.002	1.83208
15	A	W1	1.600E+08	0.002	2.035554
16	MA	W1	1.485E+08	0.002	1.674911
17	MA	W1	1.558E+08	0.002	1.899161
18	MA	W1	1.572E+08	0.002	1.944667
19	CA	W1	1.431E+08	0.002	1.519819
20	CA	W1	1.436E+08	0.002	1.533524
21	CA	W1	1.432E+08	0.002	1.52213
22	CMA	W1	1.495E+08	0.002	1.704259
23	CMA	W1	1.630E+08	0.002	2.138405
24	CMA	W1	1.447E+08	0.002	1.564447
25	A	W2	1.667E+08	0.002	2.268106
26	A	W2	1.615E+08	0.002	2.084634
27	A	W2	1.623E+08	0.002	2.113807
28	MA	W2	1.572E+08	0.002	1.942214
29	MA	W2	1.563E+08	0.002	1.915885
30	MA	W2	1.624E+08	0.002	2.116897
31	CA	W2	1.584E+08	0.002	1.981619

32	CA	W2	1.607E+08	0.002	2.059181
33	CA	W2	1.543E+08	0.002	1.850521
34	CMA	W2	1.579E+08	0.002	1.965554
35	CMA	W2	1.507E+08	0.002	1.741301
36	CMA	W2	1.510E+08	0.002	1.748073
37	A	W3	1.929E+08	0.002	3.325038
38	A	W3	1.968E+08	0.002	3.504499
39	A	W3	1.875E+08	0.002	3.085486
40	MA	W3	1.933E+08	0.002	3.343744
41	MA	W3	1.877E+08	0.002	3.092937
42	MA	W3	1.886E+08	0.002	3.133834
43	CA	W3	1.670E+08	0.002	2.278775
44	CA	W3	1.707E+08	0.002	2.4127
45	CA	W3	1.742E+08	0.002	2.543451
46	CMA	W3	1.642E+08	0.002	2.180264
47	CMA	W3	1.764E+08	0.002	2.628562
48	CMA	W3	1.761E+08	0.002	2.618404
49	A	E1	1.601E+08	0.002	2.040232
50	A	E1	1.528E+08	0.002	1.805187
51	A	E1	1.567E+08	0.002	1.929025
52	MA	E1	1.627E+08	0.002	2.12756
53	MA	E1	1.609E+08	0.002	2.067398
54	MA	E1	1.653E+08	0.002	2.218348
55	CA	E1	1.552E+08	0.002	1.879679
56	CA	E1	1.540E+08	0.002	1.840778
57	CA	E1	1.538E+08	0.002	1.834194
58	CMA	E1	1.746E+08	0.002	2.558906
59	CMA	E1	1.617E+08	0.002	2.091683
60	CMA	E1	1.590E+08	0.002	2.001663
61	A	E2	1.490E+08	0.002	1.689581
62	A	E2	1.564E+08	0.002	1.916392
63	A	E2	1.528E+08	0.002	1.803574
64	MA	E2	1.582E+08	0.002	1.975295
65	MA	E2	1.569E+08	0.002	1.932952
66	MA	E2	1.623E+08	0.002	2.113754
67	CA	E2	1.336E+08	0.002	1.269646
68	CA	E2	1.296E+08	0.002	1.172266
69	CA	E2	1.245E+08	0.002	1.053761
70	CMA	E2	1.452E+08	0.002	1.578394
71	CMA	E2	1.479E+08	0.002	1.65678
72	CMA	E2	1.488E+08	0.002	1.682264
73	A	E3	1.472E+08	0.002	1.635693
74	A	E3	1.514E+08	0.002	1.761886
75	A	E3	1.404E+08	0.002	1.446198

76	MA	E3	1.506E+08	0.002	1.736825
77	MA	E3	1.498E+08	0.002	1.712512
78	MA	E3	1.429E+08	0.002	1.514342
79	CA	E3	1.306E+08	0.002	1.196202
80	CA	E3	1.258E+08	0.002	1.082748
81	CA	E3	1.300E+08	0.002	1.181016
82	CMA	E3	1.349E+08	0.002	1.302255
83	CMA	E3	1.367E+08	0.002	1.346672
84	CMA	E3	1.375E+08	0.002	1.36732

Raw Data from KCl Elution Solution

Sample	gel type	Wash Type	Area	volume	ACh (mg)
1	A	L	1.925E+08	0.002	3.305377
2	A	L	1.844E+08	0.002	2.95341
3	A	L	1.887E+08	0.002	3.13547
4	MA	L	1.986E+08	0.002	3.585442
5	MA	L	1.994E+08	0.002	3.623618
6	MA	L	1.964E+08	0.002	3.485441
7	CA	L	1.911E+08	0.003	4.867688
8	CA	L	2.095E+08	0.003	6.189328
9	CA	L	1.793E+08	0.003	4.119066
10	CMA	L	1.833E+08	0.002	2.907674
11	CMA	L	1.737E+08	0.002	2.525762
12	CMA	L	1.827E+08	0.002	2.884122
13	A	W1	1.554E+08	0.002	1.886689
14	A	W1	1.573E+08	0.002	1.948172
15	A	W1	1.632E+08	0.002	2.143404
16	MA	W1	1.542E+08	0.002	1.848734
17	MA	W1	1.818E+08	0.002	2.846825
18	MA	W1	1.572E+08	0.002	1.943248
19	CA	W1	1.335E+08	0.002	1.266609
20	CA	W1	1.597E+08	0.002	2.024392
21	CA	W1	1.376E+08	0.002	1.371766
22	CMA	W1	1.668E+08	0.002	2.269845
23	CMA	W1	1.746E+08	0.002	2.55981
24	CMA	W1	1.632E+08	0.002	2.145526
25	A	W2	1.712E+08	0.002	2.430232
26	A	W2	1.394E+08	0.002	1.4175
27	A	W2	1.753E+08	0.002	2.586625
28	MA	W2	1.844E+08	0.002	2.952325
29	MA	W2	1.817E+08	0.002	2.841307

30	MA	W2	1.812E+08	0.002	2.821662
31	CA	W2	1.557E+08	0.002	1.893873
32	CA	W2	1.635E+08	0.002	2.154135
33	CA	W2	1.575E+08	0.002	1.952453
34	CMA	W2	1.622E+08	0.002	2.110775
35	CMA	W2	1.584E+08	0.002	1.983372
36	CMA	W2	1.616E+08	0.002	2.089729
37	A	W3	1.450E+08	0.002	1.572232
38	A	W3	1.552E+08	0.002	1.880164
39	A	W3	1.448E+08	0.002	1.566118
40	MA	W3	1.520E+08	0.002	1.778079
41	MA	W3	1.481E+08	0.002	1.6635
42	MA	W3	1.505E+08	0.002	1.734222
43	CA	W3	1.330E+08	0.002	1.2541
44	CA	W3	1.481E+08	0.002	1.661851
45	CA	W3	1.351E+08	0.002	1.305348
46	CMA	W3	1.461E+08	0.002	1.602866
47	CMA	W3	1.363E+08	0.002	1.336114
48	CMA	W3	1.403E+08	0.002	1.442376
49	A	E1	9.244E+07	0.002	0.483106
50	A	E1	1.177E+08	0.002	0.91046
51	A	E1	1.004E+08	0.002	0.599951
52	MA	E1	9.865E+07	0.002	0.572854
53	MA	E1	9.695E+07	0.002	0.547353
54	MA	E1	9.717E+07	0.002	0.550568
55	CA	E1	7.398E+07	0.002	0.269339
56	CA	E1	1.046E+08	0.002	0.668012
57	CA	E1	7.771E+07	0.002	0.306467
58	CMA	E1	8.250E+07	0.002	0.358437
59	CMA	E1	7.855E+07	0.002	0.315223
60	CMA	E1	8.126E+07	0.002	0.344516
61	A	E2	8.477E+07	0.002	0.384919
62	A	E2	9.702E+07	0.002	0.548307
63	A	E2	8.585E+07	0.002	0.397955
64	MA	E2	9.740E+07	0.002	0.554065
65	MA	E2	9.676E+07	0.002	0.544481
66	MA	E2	8.921E+07	0.002	0.440041
67	CA	E2	6.543E+07	0.002	0.195195
68	CA	E2	7.501E+07	0.002	0.279293
69	CA	E2	6.351E+07	0.002	0.180531
70	CMA	E2	7.001E+07	0.002	0.233116
71	CMA	E2	6.717E+07	0.002	0.209139
72	CMA	E2	7.401E+07	0.002	0.269639
73	A	E3	9.215E+07	0.002	0.479084

74	A	E3	1.047E+08	0.002	0.670136
75	A	E3	9.556E+07	0.002	0.527018
76	MA	E3	9.979E+07	0.002	0.590328
77	MA	E3	1.041E+08	0.002	0.659137
78	MA	E3	8.281E+07	0.002	0.361979
79	CA	E3	6.609E+07	0.002	0.200405
80	CA	E3	6.321E+07	0.002	0.178317
81	CA	E3	6.607E+07	0.002	0.200298
82	CMA	E3	7.061E+07	0.002	0.238364
83	CMA	E3	6.800E+07	0.002	0.215956
84	CMA	E3	7.309E+07	0.002	0.260969

Raw Data from Tris-HCl Elution Solution

Sample	Gel Type	Wash Type	Area	volume	ACh (mg)
1	A	L	1.798E+08	0.002	2.763825
2	A	L	1.676E+08	0.002	2.299589
3	A	L	1.657E+08	0.002	2.231472
4	MA	L	1.907E+08	0.002	3.225583
5	MA	L	1.887E+08	0.002	3.136594
6	MA	L	1.937E+08	0.002	3.360161
7	CA	L	1.885E+08	0.002	3.128258
8	CA	L	1.913E+08	0.002	3.252176
9	CA	L	1.871E+08	0.002	3.067492
10	CMA	L	1.955E+08	0.002	3.440617
11	CMA	L	1.883E+08	0.002	3.120811
12	CMA	L	1.903E+08	0.002	3.208466
13	A	W1	1.433E+08	0.002	1.525441
14	A	W1	1.520E+08	0.002	1.78039
15	A	W1	1.536E+08	0.002	1.829708
16	MA	W1	1.584E+08	0.002	1.981212
17	MA	W1	1.625E+08	0.002	2.118551
18	MA	W1	1.628E+08	0.002	2.130762
19	CA	W1	1.592E+08	0.002	2.007692
20	CA	W1	1.557E+08	0.002	1.895214
21	CA	W1	1.510E+08	0.002	1.750204
22	CMA	W1	1.586E+08	0.002	1.990565
23	CMA	W1	1.618E+08	0.002	2.097861
24	CMA	W1	1.623E+08	0.002	2.11374
25	A	W2	1.548E+08	0.002	1.866399
26	A	W2	1.549E+08	0.002	1.869048
27	A	W2	1.548E+08	0.002	1.867032

28	MA	W2	1.558E+08	0.002	1.897711
29	MA	W2	1.598E+08	0.002	2.028056
30	MA	W2	1.598E+08	0.002	2.029125
31	CA	W2	1.509E+08	0.002	1.745658
32	CA	W2	1.464E+08	0.002	1.611695
33	CA	W2	1.459E+08	0.002	1.599061
34	CMA	W2	1.506E+08	0.002	1.738057
35	CMA	W2	1.472E+08	0.002	1.634704
36	CMA	W2	1.502E+08	0.002	1.72523
37	A	W3	1.554E+08	0.002	1.885178
38	A	W3	1.552E+08	0.002	1.87832
39	A	W3	1.518E+08	0.002	1.774454
40	MA	W3	1.569E+08	0.002	1.934778
41	MA	W3	1.546E+08	0.002	1.860638
42	MA	W3	1.573E+08	0.002	1.945263
43	CA	W3	1.496E+08	0.002	1.707969
44	CA	W3	1.463E+08	0.002	1.610303
45	CA	W3	1.474E+08	0.002	1.642078
46	CMA	W3	1.503E+08	0.002	1.728237
47	CMA	W3	1.512E+08	0.002	1.753927
48	CMA	W3	1.557E+08	0.002	1.896528
49	A	E1	1.383E+08	0.002	1.389579
50	A	E1	1.328E+08	0.002	1.249193
51	A	E1	1.364E+08	0.002	1.339955
52	MA	E1	1.326E+08	0.002	1.243781
53	MA	E1	1.301E+08	0.002	1.184058
54	MA	E1	1.357E+08	0.002	1.321247
55	CA	E1	9.917E+07	0.002	0.580813
56	CA	E1	9.377E+07	0.002	0.501583
57	CA	E1	9.303E+07	0.002	0.491232
58	CMA	E1	1.022E+08	0.002	0.627715
59	CMA	E1	1.064E+08	0.002	0.698839
60	CMA	E1	1.039E+08	0.002	0.656601
61	A	E2	1.156E+08	0.002	0.868743
62	A	E2	1.103E+08	0.002	0.76776
63	A	E2	1.217E+08	0.002	0.993241
64	MA	E2	1.179E+08	0.002	0.91433
65	MA	E2	1.171E+08	0.002	0.897657
66	MA	E2	1.186E+08	0.002	0.929037
67	CA	E2	7.905E+07	0.002	0.320558
68	CA	E2	9.189E+07	0.002	0.475514
69	CA	E2	9.077E+07	0.002	0.460524
70	CMA	E2	9.466E+07	0.002	0.514039
71	CMA	E2	9.351E+07	0.002	0.497824

72	CMA	E2	8.887E+07	0.002	0.435651
73	A	E3	1.166E+08	0.002	0.888511
74	A	E3	1.176E+08	0.002	0.908584
75	A	E3	1.210E+08	0.002	0.979221
76	MA	E3	1.314E+08	0.002	1.215512
77	MA	E3	1.283E+08	0.002	1.141538
78	MA	E3	1.203E+08	0.002	0.964258
79	CA	E3	9.068E+07	0.002	0.459283
80	CA	E3	9.218E+07	0.002	0.479475
81	CA	E3	8.837E+07	0.002	0.42932
82	CMA	E3	1.013E+08	0.002	0.613352
83	CMA	E3	9.939E+07	0.002	0.584211
84	CMA	E3	1.016E+08	0.002	0.618362

Note: Loading Solutions are listed as 2mL because such little supernatant was left that 2mL DIH_2O was added to the polymers then aspirated off along with the rest of the liquid in order to be able to take loading samples, but not damage the polymers by trying to draw up liquid right on top of the polymer, which could cause puckering/tearing of the polymers.